

Geometry eigenvalues and the scalar product from recoupling theory in loop quantum gravity

Roberto De Pietri^{*}

*Dipartimento Di Fisica, Università di Parma and Istituto Nazionale di Fisica Nucleare, Sezione di Milano,
Gruppo Collegato di Parma, I-43100 Parma (PR), Italy*

Carlo Rovelli[†]

Department of Physics and Astronomy, University of Pittsburgh, Pittsburgh, Pennsylvania 15260

(Received 13 February 1996)

We summarize the basics of the loop representation of quantum gravity and describe the main aspects of the formalism, including its latest developments, in a reorganized and consistent form. Recoupling theory, in its graphical tangle-theoretic Temperley-Lieb formulation, provides a powerful calculation tool in this context. We describe its application to the loop representation in detail. Using recoupling theory, we derive general expressions for the spectrum of the quantum area and the quantum volume operators. We compute several volume eigenvalues explicitly. We introduce a scalar product with respect to which area and volume are symmetric operators, and (the trivalent expansions of) the spin network states are orthonormal. [S0556-2821(96)04516-X]

PACS number(s): 04.60.Ds, 03.70.+k

I. INTRODUCTION

We start with a citation from Penrose [1]: “My own view is that ultimately physical laws should find their most natural expression in terms of essentially combinatorial principles, that is to say, in terms of finite processes such as counting or other basically simple manipulation procedures. Thus, in accordance with such a view, some form of discrete or combinatorial space time should emerge.” The loop approach to quantum general relativity [2,3] seems to be leading precisely to a realization of such a vision of a combinatorial space-time, deriving it solely from a strict application of conventional quantum ideas to standard general relativity.¹

A number of recent advances in this direction have strengthened this hope. First of all, there is the mathematically rigorous development of the connection representation [9,14–16] which has led to recovering the loop representation formalism from a general quantization program. This approach has sharpened various loop representation results using rigorous C^* algebraic and measure theoretical techniques, and has put them on a solid mathematical footing. For a discussion of the precise relation between the two formulations of loop quantum gravity, see Refs. [17,18]. Furthermore: a simplification of the formalism due to the introduction in quantum gravity of the spin network basis [19] (see also [20,21]); the result that area [22] and volume operators [23,24] have discrete eigenvalues; the idea that in the presence of matter these eigenvalues might be taken as physical predictions on quantum geometry [25]; a Hamiltonian generating clock time evolution [26] and a tentative

perturbation scheme for computing diffeomorphism invariant transition amplitudes [27]; the extension of the theory to fermions [28] to the electromagnetic field [29,30]. This rapid development has produced a certain amount of confusion in the notation and the basics of the theory. A first aim of this paper is to bring some order in the kinematics of the loop representation formalism, by presenting the basics formulas, notations and results in a consistent and self-contained form. This allows us to insert a sign factor into the very definition of the loop representation, short-cutting sign complications of the previous formulation. In a sense, we bring to full maturity the insights of Ref. [19].

With this sign factor, loop states of the loop representation satisfy the axioms of Penrose’s “binor calculus” [31], or, equivalently, the axioms of the tangle-theoretic formulation of recoupling theory [32] for the special “classical” value $A = -1$ of the deformation parameter. This fact brings a powerful set of computational techniques at the service of quantum gravity. We describe here in detail how this calculus can be used. Calculations in loop quantum gravity were first performed using the grasping operation on single loops [3]. It was then realized, mainly in [15], that such combinatorial techniques admitted a group theoretical interpretation [su(2) representation theory admits a fully combinatorial description]. Recoupling theory is a further—and far more powerful—level of sophistication for the same calculus.

The idea that recoupling theory plays a role in loop quantum gravity has been advocated by Reisenberger [33] and by Smolin. Motivated by certain physical and mathematical considerations, Borissov, Major, and Smolin [34,35] have considered deformations of the standard loop representation theory. Recoupling theory with general values of the deformation parameter A plays a key role in the definition of these deformations. What we do here is very different in spirit: we remain within the framework of the standard loop-representation quantum general relativity (GR), and use recoupling theory merely as a computational tool.

^{*}Electronic address: depietri@vaxpr.pr.infn.it

[†]Electronic address: roveli@pitt.edu

¹For an overview of current ideas on quantum geometry, see [4–6]; for a recent overview of canonical gravity, see [7]; for introductions to loop quantum gravity, see [8–13].

Using recoupling theory, we derive general formulas for area and volume in quantum gravity. The spectrum of the area agrees with previously published results [23]. The derivation presented here is simpler and more elegant than the one in Ref. [23]. The first of our main results is a general formula for the volume. We present it here expressed in terms of $\text{su}(2)$ 6- j symbols (and related quantities). We confirm the fact that trivalent vertices have zero volume, first pointed out by Loll [24]. We explicitly compute many eigenstates for four- and five-valent vertices. Loll has computed a few of these eigenvalues in [36] using a different technique. We find agreement with the numbers published by Loll (see also [35]). We show that the absolute value and the square root that appear in the definition of the volume operator are well defined. Indeed, we show that the arguments of the absolute value are finite dimensional matrices diagonalizable and with real eigenvalues; and that the arguments of the square root are finite dimensional matrices diagonalizable and with real non-negative eigenvalues. We show in general that the eigenvalues of the volume are real and non-negative.

Finally, the technique introduced allows us to define a scalar product in the loop representation, by requiring that area and volume be symmetric, and that spin network states be orthogonal to each other — whatever the trivalent decomposition of high valence vertices we use. This is our second main result.

The structure of this paper is the following. In Sec. II, we review the basics of the Ashtekar formulation of general relativity and we define the loop variables (in the new form that leads directly to recoupling theory). In Sec. III, we derive the basic equations of the loop representation. In Sec. IV we discuss the role of recoupling theory. In Sec. V we define the spin network basis. In Sec. VI, we discuss the area operator, and in Sec. VII the volume operator. In Sec. VIII we define the scalar product. Section IX contains our conclusions.

II. LOOP VARIABLES IN CLASSICAL GR

We begin by reviewing the canonical formulation of general relativity in the real Ashtekar formalism [37–39]. This is given as follows. We fix a three-dimensional manifold M and consider two real (smooth) $\text{SO}(3)$ fields $A_a^i(x)$ and $\tilde{E}_i^a(x)$ on M . We use $a, b, \dots = 1, 2, 3$ for (abstract) spatial indices and $i, j, \dots = 1, 2, 3$ for internal $\text{SO}(3)$ indices. We indicate coordinates on M with x . The relation between these fields and conventional metric gravitational variables is as follows: $\tilde{E}_i^a(x)$ is the (densitized) inverse triad, related to the three-dimensional metric $g_{ab}(x)$ of the constant-time surface by

$$g g^{ab} = \tilde{E}_i^a \tilde{E}_i^b, \quad (2.1)$$

where g is the determinant of g_{ab} ; and

$$A_a^i(x) = \Gamma_a^i(x) - k_a^i(x), \quad (2.2)$$

where $\Gamma_a^i(x)$ is the $\text{SU}(2)$ spin connection associated to the triad and $k_a^i(x)$ is the extrinsic curvature of the three surface

(up to indices' position). Notice the absence of the i in Eq. (2.2), which yields the *real* Ashtekar connection. The real Ashtekar connection (2.2) is the natural variable for the Riemannian theory, but it can be used as the basic field for the Lorentzian theory as well, at the price of a more complicated form of the Hamiltonian constraint. Recently, Thiemann and Ashtekar [39] have argued that the most promising strategy for implementing the quantum reality conditions is to start from the real Ashtekar connection, and circumvent the difficulties due to the complicate form of the Lorentzian Hamiltonian constraint by expressing it in terms of the Riemannian Hamiltonian constraint via a generalized Wick transform (see also [40,41]). Here, we will not discuss the dynamics. Therefore our results can be significative for the Riemannian theory as well as for the Lorentzian theory. We will discuss the necessary modifications of the formalism for applying it to the complex Ashtekar connection at the end of Sec. VII.

It is useful for what follows to consider the dimensional character of the field with care. We set the dimension of the fields as follows:

$$\begin{aligned} [g_{ab}] &= L^2, & [\tilde{E}_i^a] &= L^2, \\ [A_a^i] &= \text{dimensionless}. \end{aligned} \quad (2.3)$$

The popular choice of taking the metric dimensionless is not very sensible in GR. It forces coordinates to have dimensions of a length, but the freedom of arbitrary transformations on the coordinates is hardly compatible with dimensional coordinates. Coordinates, for instance, can be angles, and assigning angles dimension of a length makes no sense. The Einstein action can be rewritten (see, for example, [8]) as

$$\begin{aligned} S &= \frac{1}{G} \int d^4x \sqrt{g} R = \frac{1}{G} \int dx^0 \int d^3x \\ &\times [-\dot{A}_a^i \tilde{E}_i^a + \dot{A}_0^i \tilde{C}_i + N^a \tilde{C}_a + N], \end{aligned} \quad (2.4)$$

where we have set

$$G = \frac{16\pi G_{\text{Newton}}}{c^3}, \quad (2.5)$$

G_{Newton} being Newton's gravitational constant, and \tilde{C}_i , \tilde{C}_a , \tilde{W} the diffeomorphism, Gauss, and Hamiltonian constraints. It follows that the momentum canonically conjugate to A_a^i is

$$p_i^a(x) = \frac{\delta S}{\delta \dot{A}_a^i(x)} = -\frac{1}{G} \tilde{E}_i^a \quad (2.6)$$

and therefore the fundamental Poisson bracket of the Hamiltonian theory is

$$\{A_a^i(x), \tilde{E}_j^b(y)\} = G \delta_a^b \delta_j^i \delta^3(x, y). \quad (2.7)$$

The spinorial version of the Ashtekar variables is given in terms of the Pauli matrices $\sigma_i, i=1, 2, 3$, or the $\text{su}(2)$ generators $\tau_i = -(i/2)\sigma_i$, by

$$\tilde{E}^a(x) = -i \tilde{E}_i^a(x) \sigma_i = 2 \tilde{E}_i^a(x) \tau_i \quad (2.8)$$

$$A_a(x) = -\frac{i}{2} A_a^i(x) \sigma_i = A_a^i(x) \tau_i. \tag{2.9}$$

$A_a(x)$ and $\tilde{E}^a(x)$ are 2×2 complex matrices. We use upper case indices $A, B, \dots = 1, 2$ for the spinor space on which the Pauli matrices act. Thus the components of the gravitational fields are $A_{aA}{}^B(x)$ and $\tilde{E}^a{}_A{}^B(x)$.

In order to construct the loop variables, we start from some definitions.

Segment. A segment γ is a continuous and piecewise smooth map from the closed interval $[0, 1]$ into M . We write $\gamma: s \mapsto \gamma^a(s)$.

Loop. A loop α is a segment such that $\alpha^a(0) = \alpha^a(1)$. Equivalently, it is a continuous, piecewise smooth map from the circle S_1 into M^3 .

Free Loop Algebra. We consider (formal) linear combinations Φ of (formal) products of loops, as in

$$\Phi = c_0 + \sum_i c_i [\alpha_i] + \sum_{jk} c_{jk} [\alpha_j][\alpha_k] + \dots, \tag{2.10}$$

where the c 's are arbitrary complex number and the α 's are loops; we denote the space of such objects as the free loop algebra $\mathcal{A}^f[\mathcal{L}]$. (See also [9].)

Multiloop. We denote the monomials in $\mathcal{A}^f[\mathcal{L}]$, namely the elements of the form $\Phi = [\alpha_1] \dots [\alpha_n]$ as multiloops.

We indicate multiloops by a Greek letter, in the same manner as (single) loops: $[\alpha] = [\alpha_1] \dots [\alpha_n]$.

Given a segment γ , we consider the parallel propagator of A_a along γ . This is defined by the equation

$$\frac{d}{d\tau} U_\gamma(\tau, \tau_0) + \frac{d\gamma^a(\tau)}{d\tau} A_a(\gamma(\tau)) U_\gamma(\tau, \tau_0) = 0, \tag{2.11}$$

with the boundary condition $U_\gamma(\tau_0, \tau_0)_A^B = \delta_A^B$. The formal solution is

$$U_\gamma(\tau, \tau_0) = \mathcal{P} \exp \left(- \int_{\tau_0}^{\tau} d\tau \dot{\gamma}^a A_a(\gamma(\tau)) \right), \tag{2.12}$$

where \mathcal{P} indicates the path ordering of the exponential. We also write—in a somewhat imprecise notation— $U_\gamma = U_\gamma(0, 1)$ and $U_\gamma(s_2, s_1) = U_\gamma(\tau_2, \tau_1)$ if $s_2 = \gamma(\tau_2)$ and $s_1 = \gamma(\tau_1)$.

We can now define the fundamental loop variables. Given a loop α and the points $s_1, s_2, \dots, s_n \in \alpha$ we define

$$\mathcal{T}[\alpha] = -\text{Tr}[U_\alpha], \tag{2.13}$$

$$\mathcal{T}^a[\alpha](s) = -\text{Tr}[U_\alpha(s, s) \tilde{E}^a(s)] \tag{2.14}$$

and, in general,

$$\mathcal{T}^{a_1 a_2}[\alpha](s_1, s_2) = -\text{Tr}[U_\alpha(s_1, s_2) \tilde{E}^{a_2}(s_2) U_\alpha(s_2, s_1) \tilde{E}^{a_1}(s_1)], \tag{2.15}$$

$$\mathcal{T}^{a_1 \dots a_N}[\alpha](s_1, \dots, s_N) = -\text{Tr}[U_\alpha(s_1, s_N) \tilde{E}^{a_N}(s_N) U_\alpha(s_N, s_{N-1}) \dots U_\alpha(s_2, s_1) \tilde{E}^{a_1}(s_1)].$$

The function $\mathcal{T}[\alpha]$ defined in Eq. (2.13) for a single loop, can be defined over the whole free loop algebra $\mathcal{A}^f[\mathcal{L}]$: given the generic element $\Phi \in \mathcal{A}^f[\mathcal{L}]$ in Eq. (2.10), we pose

$$\mathcal{T}[\Phi] = -2c_0 + \sum_i c_i \mathcal{T}[\alpha_i] + \sum_{ij} c_{ij} \mathcal{T}[\alpha_i] \mathcal{T}[\alpha_j] + \dots \tag{2.16}$$

The reason for the -2 in the first term is the following. We may think of the first term of the sum as corresponding to the ‘‘point loop,’’ or a loop whose image is a point. For this loop, the exponent in Eq. (2.12) is zero, the holonomy is the identity [in $\mathfrak{sl}(2, C)$, namely in two dimensions] and \mathcal{T} is therefore -2 .

Notice that there is a sign difference between the usual loops observables [2,3] (denoted T variables) and these new loop observables, denoted \mathcal{T} variables. This is a key technicality at the origin of the simplification of the formalism presented here. The new sign takes care immediately of the sign complications extensively discussed in Ref. [19]. The suggestion that those sign complications could be avoided by inserting a minus sign in front of the trace was considered by Major as well [42]. Let us illustrate the consequences of having this sign. Consider an N component multiloop $\alpha = \alpha_1 \alpha_2 \dots \alpha_N$. We have

$$\begin{aligned} \mathcal{T}[\alpha_1] \dots [\alpha_N] &= \mathcal{T}[\alpha_1] \dots \mathcal{T}[\alpha_1] \\ &= (-\text{Tr}[U_{\alpha_1}]) \dots (-\text{Tr}[U_{\alpha_N}]) \\ &= (-1)^N \text{Tr}[U_{\alpha_1}] \dots \text{Tr}[U_{\alpha_N}] \\ &= (-1)^N \mathcal{T}[\{\alpha\}]. \end{aligned}$$

This shows that the new sign choice implements in the formalism the sign factor for the number of loops that was recognized in [19] as the key to transform the spinor relation into a local relation. In fact, we have

$$\text{Tr}[U_\alpha] \text{Tr}[U_\beta] - \text{Tr}[U_\alpha U_\beta] - \text{Tr}[U_\alpha U_{\beta^{-1}}] = 0, \tag{2.17}$$

$$\mathcal{T}[\alpha] \mathcal{T}[\beta] + \mathcal{T}[\alpha \#_s \beta] + \mathcal{T}[\alpha \#_s \beta^{-1}] = 0, \tag{2.18}$$

$$\mathcal{T}[\alpha][\beta] + \mathcal{T}[\alpha \#_s \beta] + \mathcal{T}[\alpha \#_s \beta^{-1}] = 0; \tag{2.19}$$

namely the spinor identity (one $+$ and two $-$) has become a binor identity (all $+$) (see Penrose [43]). While the first is nonlocal, the second is local, and is the basic identity at the roots of binor calculus and $A = -1$ recoupling theory. For the notations \circ and $\#$ (to be used in a moment), see for instance [8].

We recall here, for later use, the retracing identity. For all loops α and segments γ , we have [3]

$$\mathcal{T}[\alpha] = \mathcal{T}[\alpha \circ \gamma \circ \gamma^{-1}]. \quad (2.20)$$

The Poisson bracket algebra of these loop variables is easily computed. For a rigorous way of performing these computations, see [44]. We give here the Poisson bracket of the \mathcal{T} variables of order 0 and 1.

$$\{\mathcal{T}[\alpha], \mathcal{T}[\beta]\} = 0, \quad (2.21)$$

$$\{\mathcal{T}^a[\alpha](s), \mathcal{T}[\beta]\} = -\frac{1}{2} G \Delta^a[\beta, s] \{\mathcal{T}[\alpha \#_s \beta] - \mathcal{T}[\alpha \#_s \beta^{-1}]\}, \quad (2.22)$$

where we have defined

$$\Delta^a[\beta, s] = \int_{\beta} d\tau \dot{\beta}^a(\tau) \delta^3[\beta(\tau), s]. \quad (2.23)$$

The factor $-\frac{1}{2}$, different than in previous papers, is due to the new conventions.

III. THE LOOP REPRESENTATION OF QUANTUM GRAVITY

We now define the loop representation [45] of quantum gravity as a linear representation of the Poisson algebra of the \mathcal{T} variables. First, we define the carrier space of the representation. To this aim, we consider the linear subspace \mathcal{K} of the free loop algebra defined by

$$\mathcal{K} = \{\Phi \in \mathcal{A}^f[\mathcal{L}] | \mathcal{T}[\Phi] = 0\}, \quad (3.1)$$

and we define the carrier space \mathcal{V} of the representation by

$$\mathcal{V} = \mathcal{A}^f[\mathcal{L}] / \mathcal{K}. \quad (3.2)$$

In other words, the state space of the loop representation is defined as the space of the equivalence classes of linear combinations of multiloops, under the equivalence defined by the Mandelstam relations

$$\Phi \sim \Psi \quad \text{if} \quad \mathcal{T}[\Phi] = \mathcal{T}[\Psi], \quad (3.3)$$

namely by the equality of the corresponding holonomies [9].² We denote the equivalence classes defined in his way, namely the elements of the quantum state space of the theory as Mandelstam classes, and we indicate them in Dirac notation as $\langle \Phi |$. Clearly, the multiloop states $\langle \alpha |$ span (actually, overspan) the state space \mathcal{V} . Later we will define a scalar product on \mathcal{V} , and promote it to a Hilbert space. The reason for preferring a bra notation over a ket notation is just historical at this point. We recall that the loop representation

was originally defined in terms of kets $|\psi\rangle$ in the dual of \mathcal{V} . These are represented on the (overcomplete) basis $\langle \alpha |$ by loop functionals

$$\psi(\alpha) = \langle \alpha | \psi \rangle. \quad (3.4)$$

The principal consequences of the Mandelstam relations are the following:

(1) The element $\langle \alpha |$ does not depend on the orientation of α , $[\alpha] \sim [\alpha^{-1}]$; (2) the element $\langle \alpha |$ does not depend on the parametrization of α , $[\alpha] \sim [\beta]$ if $\beta^a(\tau) = \alpha^a(f(\tau))$; (3) retracing, if γ is a *segment* starting in a point of α , then

$$[\alpha \circ \gamma \circ \gamma^{-1}] \sim [\alpha]; \quad (3.5)$$

(4) the binor identity

$$[\alpha] \cdot [\beta] \sim -[\alpha \#_s \beta] - [\alpha \#_s \beta^{-1}]. \quad (3.6)$$

It has been conjectured that all Mandelstam relations can be derived by repeated use of these identities. We expect that the methods described below may allow to prove this conjecture, but we do not discuss this issue here.

Next, we define the quantum operators corresponding to the \mathcal{T} variables as linear operators on \mathcal{V} . These form a representation of the loop variables Poisson algebra. We define the loop operators as acting on the bra states $\langle \Phi |$ from the right. (Since they act on the right, they define, more precisely, an *antirepresentation* of the Poisson algebra.) We define the $\hat{\mathcal{T}}[\alpha]$ operator by

$$\begin{aligned} & \left\langle c_0 + \sum_i c_i [\alpha_i] + \sum_{ij} c_{ij} [\alpha_i] [\alpha_j] + \dots \right| \hat{\mathcal{T}}[\alpha] \\ &= \left\langle c_0 [\alpha] + \sum_i c_i [\alpha_i] [\alpha] + \sum_{ij} c_{ij} [\alpha_i] [\alpha_j] [\alpha] + \dots \right|. \end{aligned} \quad (3.7)$$

Next, we define the $\hat{\mathcal{T}}^a[\alpha](s)$ operator. This is a derivative operator (i.e., it satisfies Leibniz rule) over the free loop algebra such that

$$\langle [\beta] | \hat{\mathcal{T}}^a[\alpha](s) = -\frac{1}{2} i l_0^2 \Delta^a[\beta, s] (\langle [\alpha \#_s \beta] | - \langle [\alpha \#_s \beta^{-1}] |), \quad (3.8)$$

where we have introduced the elementary length l_0 by

$$l_0^2 = \hbar G = \frac{16\pi\hbar G_{\text{Newton}}}{c^3} = 16\pi l_{\text{Planck}}^2. \quad (3.9)$$

The definition extends on the entire free loop algebra by Leibniz rule and linearity. The two operators commute with the Mandelstam relations and are therefore well defined on \mathcal{V} .

Notice that the factor $\Delta^a[\beta, s]$ in Eq. (3.8) depends on the orientation of the loop β : it changes sign if the orientation of β is reversed. So does the difference in the parentheses, therefore the right-hand side (rhs) of Eq. (3.8) is independent from the orientation of β , as the lhs. On the other hand, both

² $\mathcal{T}[\Phi]$ is a function on configuration space, namely a function over the space of smooth connections. Equality between functions means of course having the same value for any value of the independent variable; here, for all (smooth) connections.

the rhs and the lhs of Eq. (3.8) change sign if we reverse the orientation of α .

The action of the $\hat{T}^a[\alpha](s)$ operator on a state $\langle[\beta]|$ can be visualized graphically. The graphical action is denoted a ‘‘grasp,’’ and it can be described as follows. (i) Disjoin the two edges of the loop β and the two edges of the loop α , that enter the intersection point s . (ii) Pairwise join the four open ends of α and β in the two possible alternative ways. This defines two new states. Consider the difference between these two states (arbitrarily choosing one of the two as positive). (iii) Multiply this difference by the factor $-il_0^2\Delta^a[\beta,s]$, where the direction of β (which determines the sign of $\Delta^a[\beta,s]$) is determined as follows: it is the direction induced on β by α (which is oriented) in the term chosen as positive. A moment of reflection shows that the definition is consistent, and independent from the choice of the positive term. An explicit computation shows that the operators defined realize a linear representation of the Poisson algebra of the corresponding classical observables.

The grasping rule generalizes to higher order \mathcal{T} variables. The action of $\hat{T}^{a_1\cdots a_n}[\alpha](s_1, \dots, s_n)$, over a single loop-state $[\beta]$ is given as follows. First the result vanishes unless β crosses all the n points s_i . If it does, the action of $\hat{T}^{a_1\cdots a_n}[\alpha](s_1, \dots, s_n)$ is given by the simultaneous grasp on all intersection points. This action produces 2^n terms. These terms are summed algebraically with alternate signs, and the result is multiplied by a factor $-il_0^2\Delta^a[\beta,s_i]$ for each grasp, where the sign of each coefficient $\Delta^a[\beta,s_i]$ is determined assuming that β is oriented consistently with α in the term chosen as positive. Again, a moment of reflection shows that the definition is consistent, and independent from the choice of the positive terms. The generalization to arbitrary states, using linearity and the Leibnitz rule, is straightforward. This concludes the construction of the linear ingredients of the loop representation.

IV. LOOP STATES AND RECOUPLING THEORY

A quantum state $\langle\Phi|$ in the state space \mathcal{V} is a Mandelstam equivalence class of elements of the form (2.10). We now show that because of the equivalence relation, these states are related to tangles—in the sense of Kauffman [46]—and they obey the formal identities that define the Temperley-Lieb-Kauffman recoupling theory described in Ref. [32]. This fact yields two results. First, we can write a basis in \mathcal{V} . This basis is constructed in the next section. Second, recoupling theory becomes a powerful calculus in loop quantum gravity.

Consider the element Φ , given in Eq. (2.10), of the vector space $\mathcal{A}^f[\mathcal{L}]$. We need some definitions.

Graph of a state. We denote the union in M of the images of all the loops in the rhs of Eq. (2.10) as the ‘‘graph of Φ ,’’ and we indicate it as Γ_Φ . Notice that Γ_Φ is a graph in the sense of graph theory [47], embedded in M .

Vertex. We denote the points i where Γ_Φ fails to be a smooth submanifold of M as ‘‘vertices.’’

Edge. We denote the lines e of the graph connecting the vertices as ‘‘edges.’’

Valence. We say that a vertex i has valence n , or is n valent, if n edges are adjacent to it. A vertex can have any positive integer valence, including 1 and 2.

Clearly, Φ is not uniquely determined by its graph Γ_Φ . If our only information about a state is its graph, then we do not know how the state is decomposed into multiloops, nor how many single loops run along each edge, nor how the single loops are rooted through the vertices. We now introduce a graphical technique to represent this missing information. The technique is based on the idea of ‘‘blowing up’’ the graph—as if viewed through an infinite magnifying glass—and representing the additional information in terms of planar tangles on the blown up graph. As we will see, these tangles obey recoupling theory.

First, draw a graph isomorphic to Γ_Φ in the sense of graph theory (that is, the isomorphism preserves only adjacency relations between vertices and edges), on a two-dimensional surface. As usual in graph theory, we must distinguish points representing vertices from accidental intersections between edges generated by the fact that we are representing a non-planar graph on a plane. Denote these accidental intersections as ‘‘false intersections.’’ Next, replace each vertex (not the false intersections) by (the interior of) a circle in the plane, and each edge by a ribbon connecting two circles. (At false intersections, ribbons bridge each other without merging.) In this way, we construct a ‘‘thickened out’’ graph: a two-dimensional oriented surface which (loosely speaking) has the topology of the graph Γ_Φ times the $[0,1]$ interval.

Ribbon-net. We call this two-dimensional surface the ‘‘ribbon net’’ (or simply the ribbon) of the graph Γ_Φ , and we denote it as R_Φ . Notice that the graph Γ_Φ is embedded in M , while its ribbon net R_Φ is not.

Now we can represent the missing information needed to reconstruct Φ from Γ_Φ as (a formal linear combination of) tangles drawn on the surface R_Φ . First, we represent each multiloop in Eq. (2.10) by means of a closed line over R_Φ :

Planar (representation of a) multiloop. For each loop α_i in a given multiloop α we draw a loop α_i over the ribbon net R_Φ , wrapping around R_Φ in the same way in which α_i wraps around Γ_Φ . We denote the drawing (over R_Φ) of all the loops of a multiloop as ‘‘the planar representation’’ of the multiloop α , or simply as the ‘‘planar multiloop.’’ We indicate it as P_α .

For technical reasons, we allow edges and vertices of the ribbon net to be empty of loops as well. Thus we identify a ribbon net containing a planar multiloop, with a second one obtained from the first by adding edges and vertices empty of loops. Finally:

Planar (representation of a) state. Every state $\langle\Phi|$ is a formal linear combination of multiloops: $\langle\Phi| = \sum_j c_j [\alpha_j]$ (up to equivalence). We denote the corresponding formal linear combination $P_\Phi = \sum_j c_j P_{\alpha_j}$ of planar multiloops on the ribbon net R_Φ (up to equivalence), as a planar representation of $\langle\Phi|$.

We have split the information contained in Φ in two parts: Φ determines a graph Γ_Φ embedded in M and a planar state P_Φ . P_Φ is a linear combinations of drawings of loops over a surface (the ribbon net R_Φ) and codes the information on which loops are present and how they are rooted through intersections. This information is *purely combinatorial*. On

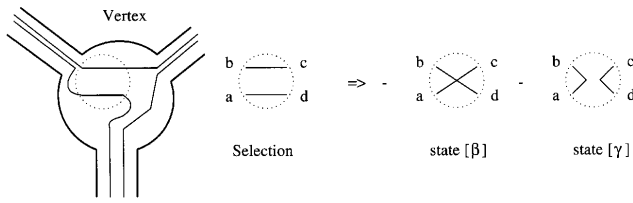


FIG. 1. The binor identity.

the other hand, Γ_Φ contains the information on how the loops are embedded into M .

Notice that a multiloop determines its planar representation only up to smooth planar deformations of the lines within the circles and the ribbons of the ribbon net. In other words, we can arbitrarily deform the lines within each circle and within each ribbon, without changing Φ . In particular, the lines of the planar representation will intersect in points of R_Φ , and we can apply Reidemeister [48] moves [46] to such intersections (that is, disentangle them). Under and overcrossings of loops within R_Φ are not distinguished.

Let us come to the key observation on which the possibility of using recoupling theory relies. Consider an element Φ of the free vector algebra. For simplicity, let us momentarily assume that Φ is formed by a single loop $\Phi = [\alpha]$ (which may self-intersect and run over itself). Thus $\Phi = (\Gamma_\alpha, P_\alpha)$. Consider an intersection of two lines (two segments of P_α) in R_Φ . Break the two lines meeting at this intersection, and pairwise rejoin the four legs, in the two alternative possible ways, as in Fig. 1.

We obtain two new loops on R_Φ , which we denote as $P_{[\beta]}$ and $P_{[\gamma]}$. Consider the element Ψ of the free vector algebra uniquely determined by the graph $\Gamma_\Psi = \Gamma_\Phi$, and by the linear combination of planar representations $P_\Psi = -P_\beta - P_\gamma$. Notice that Ψ is different than Φ as an element of the free vector algebra; however, the two are in the same Mandelstam equivalence class because of the binor relation (3.6), and therefore they define the same element of the quantum state space \mathcal{V} . Namely $\langle \Psi | = \langle \Phi |$. We say that two planar representations P_Φ and P_Ψ are “equivalent” if $\langle \Psi | = \langle \Phi |$. Thus, in dealing with planar representations of a quantum state $\langle \Phi |$, we can freely use the identity

$$\times = - | | - \cup \tag{4.1}$$

on P_Φ without changing the quantum state. This identity is the identity (i) in p. 7 of Ref. [32] [Eq. (B1) in Appendix B], which is the key axiom of recoupling theory — with the value of the A parameter set to -1 .

An easy to derive consequence is that every closed line entirely contained within a circle, or within a ribbon, can be replaced by a factor $d = -2$. Furthermore, it is easy to see that the retracing identity (3.5) implies that the loops of P_Φ can be arbitrarily deformed within the *entire* ribbon net, without changing the state $\langle \Phi |$. In particular, every loop contractible in R_Φ can be replaced by a factor $d = -2$. This is

the second axiom of recoupling theory [Eq. (B2) in Appendix B] in the $A = -1$ case. The value $A = -1$, correspond to the case in which the distinction between over and undercrossings can be neglected, consistently with the fact such distinction is irrelevant for the planar representation of a loop.

Thus P_Φ can be interpreted as a linear combination of tangles in the sense of Ref. [32]. The tangles obey the axioms of recoupling theory. They are confined inside the oriented surface R_Φ with has a highly nontrivial topology. This is the key result of this section.

The relation between loop states and recoupling theory is subtle, and may generate confusion. A source of confusion is given by the fact that the relation between recouplings and knots in knot theory [32] is different from the relation between recouplings and knots in quantum gravity. In both cases recouplings enters as a consequence of a skein (or binor) equation — as Eq. (4.1) — holding at intersections. But in knot theory this equation is satisfied by the Kauffman brackets at the “false intersections” of the planar projection of a loop. Contrary to this, in quantum gravity Eq. (4.1) *does not hold* for the false intersections. It holds for the intersections of lines *within* R_Φ .

On the other hand, knots play a role in quantum gravity as well [2], because of the diffeomorphism constraint. GR’s diffeomorphism invariance identifies states that have equivalent P_Φ , and whose *graphs* can be deformed into each other by 3D diffeomorphism of M in the connected component of the identity. To clarify this point, let us require that the ribbon net R_Φ is generated by a two-dimensional projection of Γ_Φ , and let us keep track of the resulting over and undercrossings at false intersections. Then diffeomorphism invariance identifies all states that have equivalent P_Φ , and whose ribbon nets can be transformed into each other by Reidemeister moves *at the false intersections*. Thus, as far as diff-invariant states are concerned, Reidemeister moves can be used at the tangles’ intersections *within the ribbon net* as well as at the false intersections. But in the first case a skein equation [Eq. (4.1)] holds, in the second it does not.³ Mixing up the two cases has generated a certain confusion in the past.

An immediate consequence of the result is that we can write a basis in \mathcal{V} following [32]. Given a state $\langle \Psi |$, and its ribbon net R_Φ , we can use Eq. (4.1) to eliminate all intersections from the P_α of each multiloop. Next, we can retrace each single line that returns over itself, and eliminate every loop contractible in R_Φ . We obtain parallel lines without intersections along each ribbon and routings without intersections at each vertex. No further use of the retracing or binor identity is then possible without altering this form. This procedure defines a basis of independent states, labeled by the graph, the number of lines along each edge, and elementary routings at each node. An elementary routing is a planar rooting of loops through the vertex of the ribbon net,

³This is true in general. One may wonder if there is any special quantum state $\langle \Phi_0 |$ for which the relation (4.1) holds at false intersections as well. The possibility that such a special state could exist in quantum gravity has been explored, with various motivations, by various authors [34,49].

having no intersections. This basis is not very practical for calculations. In the next section, we use the technology of [32] to define a more useful basis.⁴

V. THE SPIN NETWORK BASIS

The representation (Γ_Φ, P_Φ) of a state $\langle \Phi |$ can be expanded in terms of a “virtual” trivalent representation as follows.

Virtual graph. To every graph Γ , we can associate a trivalent graph Γ^v as follows. For each n -valent vertex v of Γ , (arbitrarily) label the adjacent edges as $e_0 \dots e_{(n-1)}$, and disjoint them from v . Then, replace v with $n-2$ trivalent vertices $N_1 \dots N_{n-2}$, denoted “virtual” vertices. Join the virtual vertices with $n-3$ “virtual” edges $E_2 \dots E_{n-2}$, where E_i joins N_{i-1} and N_i . Prolong the edges $e_2 \dots e_{(n-1)}$ to reach the corresponding virtual vertices $N_1 \dots N_{n-2}$, and the edges e_1 and $e_{(n-1)}$ to reach the virtual vertices N_1 and N_{n-2} . Denote the resulting trivalent graph Γ^v as the virtual graph associated to Γ (for the chosen ordering of edges).

Virtual ribbon net. We denote the ribbon net of Γ_Φ^v as the virtual ribbon net R_Φ^v of Φ . We view it as a subset of R_Φ , namely we view the virtual circles $N_1 \dots N_{n-2}$ and the virtual ribbons $E_2 \dots E_{n-2}$ as drawn inside the circle c representing v . This circle c indicates that the virtual vertices $N_1 \dots N_{n-2}$ correspond all to the same point of M . (Thus a virtual ribbon net is a trivalent ribbon net with strings of adjacent intersections specified.)

Virtual representation. Finally, deform P_Φ so that it lies entirely inside R_Φ^v . We indicate the deformed P_Φ as P_Φ^v and call it the “virtual” planar representation of Φ . The virtual representation P_Φ^v of a state is not unique, due to the arbitrariness of assigning the ordering $e_0 \dots e_{(n-1)}$ to the edges of n -valent intersections.

The above construction is more difficult to describe in words than to visualize, and is illustrated in Fig. 2.

Consider now deformations of the tangle P_Φ^v within R_Φ^v —a subset of the deformations within the full R_Φ . We can move all intersections of deform P_Φ^v away from the vertices (to the virtual or real ribbons), leaving trivalent vertices free from intersections. Next, we can use the binor relation to remove all intersections from the ribbons, leaving noninter-

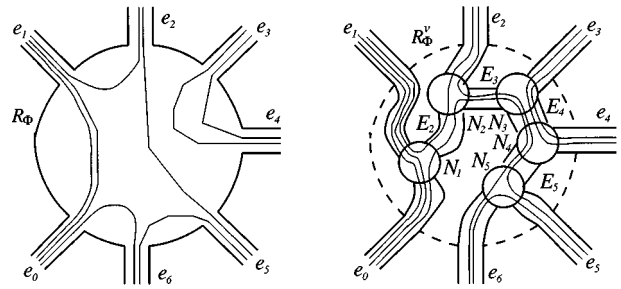


FIG. 2. Construction of “virtual” vertices and “virtual” strips over an n -valent vertex.

secting tangles with n inputs and n outputs along each single ribbon e . As described in Sec 2.2 of [32], tangles of this kind can be described as elements of the (tangle-theoretic) Temperley-Lieb algebras $T_n^{(e)}$. A basis of this algebra is obtained by using the Jones-Wenzl projectors $\Pi_n^{(e)}$. Since we are here in the case $A = -1$, the $\Pi_n^{(e)}$ are just normalized antisymmetrizers. More precisely, given the multiloop P_α with n lines along the ribbon e , call $P_\alpha^{(p)}$, $p = 1 \dots n!$ the multiloops obtained by all possible permutations p in the way the n lines entering e are connected to the n outgoing lines, and $|p|$ the parity of the permutation, then

$$\Pi_n^{(e)} P_\alpha = \frac{1}{n!} \sum_p (-1)^{|p|} P_\alpha^{(p)}. \tag{5.1}$$

Notice the $1/n!$ factor, which was not present in previous conventions [23]. It follows from the completeness of the Jones-Wenzl projectors that a basis for all planar loops over a given R_Φ^v is given by the linear combination of loops in which the lines along each (virtual and real) edge are fully antisymmetrized. We can therefore expand every state in states in which lines are fully antisymmetrized along each ribbon. A state in which the lines along each (virtual or real) ribbon are fully antisymmetrized is a spin network state. Thus we recover the result of Ref. [19], to which we refer for details.

A spin network state is characterized by a graph Γ in M , by the assignment of an ordering to the edges adjacent to each vertex, and by the number p_e of (antisymmetrized) lines in each virtual or real edge e . We denote the integer p_e as the “color” of the corresponding edge e of Γ^v . We will use also the “spin” j_e of the edge, defined as half its color: $j_e = \frac{1}{2} p_e$.⁵ At each vertex, the colors p_1, p_2 , and p_3 of the three adjacent edges satisfy a compatibility condition: there must exist three positive integers a, b , and c (the number of lines rooted through each pair of edges) such that

$$p_1 = a + b, \quad p_2 = b + c, \quad p_3 = c + a. \tag{5.2}$$

⁴A basis in a linear space is a set of linearly independent vectors that span the linear space. The fact that for the moment we are still working in linear spaces without fixing a scalar product (we will fix a scalar product only later, in Sec. VIII) has raised some confusion in the past. It is perhaps worthwhile recalling that the notions of basis, eigenvalues and eigenvectors are well defined notions for linear spaces, not just for Hilbert spaces. (They do not require a scalar product to be defined in order to make sense.) Similarly, the fact that a linear operator is diagonalizable, or has real eigenvalues does not depend on the presence of a scalar product. Given an arbitrary linear basis v_i in a finite dimensional linear space, a linear operator A is Hermitian in this basis if its matrix elements [defined by $(Av)_i = A^j_i v_j$] satisfy $A^j_i = \overline{A^i_j}$. If A is Hermitian in a basis, then A is diagonalizable and has real eigenvalues. This is true independently from any scalar product.

⁵The oscillation between the historically motivated half integer terminology “spin” and the rationally motivated integer terminology “color” goes back to Penrose’s papers on spin networks [43].

It is easy to see that this condition is equivalent to the Clebsh-Gordon condition that each of the three $\mathfrak{su}(2)$ representations of spin $j_i = 1/2 p_i$ is contained in the tensor product of the other two [43].

The spin network states form a basis in \mathcal{V} . The basis elements are given as follows. For every graph Γ embedded in M , choose an ordering of the edges at each node. This choice associates an oriented trivalent virtual graph Γ^v (nonembedded) to every Γ .

Spin network. A spin network S is given by a graph Γ_S in M , and by a compatible coloring $\{p_e\}$ of the associated oriented trivalent virtual graph Γ^v . Thus $S = (\Gamma_S, \{p_e\})$.

Spin network state. For every spin network S , the spin network quantum state $\langle S | = (\Gamma_S, P_S)$ is the element of \mathcal{V} determined by the graph Γ_S and by the linear combination P_S of planar multiloops obtained as follows. Draw p_e lines on each ribbon e of the ribbon net R_S^v ; connect lines at intersections without crossings; this gives a planar multiloop $P_S^{(0)}$ then

$$P_S = \prod_{e \in \Gamma} \Pi_{p_e}^{(e)} P_S^{(0)}. \tag{5.3}$$

We can represent a spin network state as a colored trivalent graph over the ribbon net R_S^v (with a single edge along each ribbon). This representation satisfies the identities of recoupling theory. We describe the main ones of these identities in Appendix E. As an example, we give here the formula that allows one to express the basis elements of a four-valent intersection in terms of the basis elements of a different trivalent expansion. Using the recoupling theorem of [32] (p. 60), we have, immediately,

$$\begin{array}{c} b \\ \diagdown \\ \text{---} j \text{---} \\ \diagup \\ a \end{array} \begin{array}{c} c \\ \diagup \\ \text{---} \\ \diagdown \\ d \end{array} = \sum_i \left\{ \begin{array}{ccc} a & b & i \\ c & d & j \end{array} \right\} \begin{array}{c} b \\ \diagdown \\ \text{---} i \text{---} \\ \diagup \\ a \end{array} \begin{array}{c} c \\ \diagup \\ \text{---} \\ \diagdown \\ d \end{array} \tag{5.4}$$

where the quantities $\left\{ \begin{array}{ccc} a & b & i \\ c & d & j \end{array} \right\}$ are $\mathfrak{su}(2)$ six- j symbols (normalized as in [32]; see Appendices).

A side remark should be added. An embedded colored trivalent graph specify a state Φ only up to a global sign, because it does not fix the overall sign of the antisymmetrized linear combination of multiloops. To keep track of this overall sign, one needs *oriented* trivalent graphs, as in Ref. [43] where Penrose considered oriented spin networks and in [19]. An orientation of a trivalent graph is an assignment of a cyclic order to the edges of each node, modulo Z_2 (that is, identifying two orientations if they differ in an even number of intersections). Γ^v is oriented by the order assigned to the edges entering each vertex, and ribbon-nets are oriented (consistently, we assume) as graphs because they are oriented as two-surfaces: edges can be ordered, say, clockwise.

The action of the operators in the spin-network basis

We now describe how the \hat{T} operators act on the spin network states. From Eq. (3.7), the operator $\hat{T}[\alpha]$, acting on a state $\langle \Phi |$ simply adds a loop to $\langle \Phi |$. Consider the graph Γ formed by the union (in M) of the graphs of Φ and α . Since we admit empty edges, we can represent Φ over the

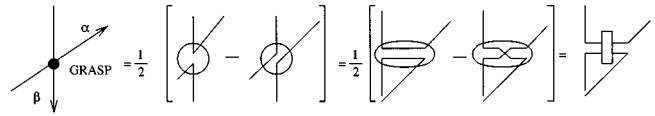


FIG. 3. Action of the grasp.

ribbon net R associated to Γ . In this representation, the action of $\hat{T}[\alpha]$ consists in adding the draw of α over R . Using the expression for the Jones-Wenzl projectors in [32] (p. 96), one can expand the nonantisymmetrized lines, if any, in combinations of antisymmetrized ones.

Higher order loop operators are expressed in terms of the elementary grasp operation, Eq. (3.8). The ribbon construction allows us to represent the grasp operation in a simpler form. Indeed, one easily sees that Eq. (3.8) is equivalent to the following: acting on an edge with color 1, the grasp creates two virtual trivalent vertices (inside the same circle, corresponding to the intersection point) — one on the spin-network state and one the loop of the operator. The two vertices are joined by a virtual strip of color 2, and the overall multiplicative factor is determined as follows. The sign of the tangent of β in $\Delta^a[\beta, s]$ is determined by the orientation of β consistent with the positive terms of the loop expansion of the spin network. The equivalence between the old definition of the grasp and the new one is illustrated in Fig. 3.

A straightforward computation, using Leibnitz rule, shows that acting on an edge with color p , the grasp has the very same action, with the multiplicative factor multiplied by p . Finally, notice that the two antisymmetrized loops form a (virtual) spin network edge of color 2. Therefore, we can express the action of the grasp in the spin network basis by the following equation:

$$\begin{array}{c} \beta \\ \downarrow \\ \text{---} s \text{---} \\ \uparrow \\ p \end{array} \begin{array}{c} \alpha \\ \diagup \\ \text{---} \\ \diagdown \end{array} \text{GRASP} = p \Delta^a[\beta, s] \begin{array}{c} R_\Phi \\ \uparrow \\ \text{---} p \text{---} \\ \downarrow \\ \text{---} \\ \uparrow \\ p \end{array} \begin{array}{c} \alpha \\ \diagup \\ \text{---} \\ \diagdown \\ 1 \end{array} \tag{5.5}$$

This simple form of the action of the loop operators on the spin-network basis is the reason that enables us to use recoupling-theory in actual calculations involving quantum gravity operators. Notice that it is the ribbon-net construction that allows us to “open up” the intersection point and represent it by means of two vertices (one over α and one over β) and a (“zero length”) edge connecting the two vertices. These two vertices and this edge are all in the same point of the three-manifold M .

Higher order loop operators act similarly, as sketched in Fig. 4.

VI. THE AREA OPERATOR

A surface Σ in M is an embedding of a two-dimensional manifold Σ , with coordinates $\sigma^\mu = (\sigma^1, \sigma^2), u, v = 1, 2$, into M . We write $S: \Sigma \rightarrow M^3, \sigma^\mu \rightarrow x^\alpha(\sigma)$. The metric and the normal one form on Σ are given by

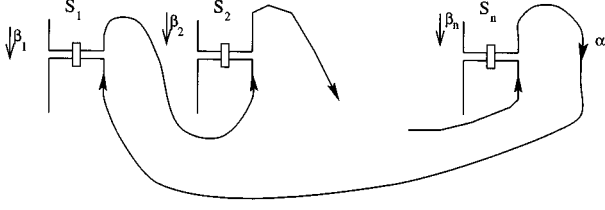


FIG. 4. Representation of the n grasp of the $\mathcal{T}^{a_1 \dots a_n}[\alpha](s_1, \dots, s_n)$ operator.

$$g^\Sigma = S^* g, \quad g_{uv}^\Sigma = \frac{\partial x^a}{\partial \sigma^u} \frac{\partial x^b}{\partial \sigma^v} g_{ab}; \quad (6.1)$$

$$n_a = \frac{1}{2} \epsilon^{uv} \epsilon_{abc} \frac{\partial x^b}{\partial \sigma^u} \frac{\partial x^c}{\partial \sigma^v}. \quad (6.2)$$

The area of Σ is

$$\begin{aligned} A[\Sigma] &= \int_\Sigma d^2 \sigma \sqrt{\det g^\Sigma} = \int_\Sigma d^2 \sigma \sqrt{\frac{1}{2} \epsilon^{u\bar{u}} \epsilon^{v\bar{v}} g_{uv}^\Sigma g_{\bar{u}\bar{v}}^\Sigma} \\ &= \int_\Sigma d^2 \sigma \sqrt{n_a n_b \tilde{E}^{a\bar{i}} \tilde{E}^{b\bar{i}}}, \end{aligned} \quad (6.3)$$

where we have used

$$\begin{aligned} \epsilon^{u\bar{u}} \epsilon^{v\bar{v}} g_{uv}^\Sigma g_{\bar{u}\bar{v}}^\Sigma &= \epsilon^{u\bar{u}} \epsilon^{v\bar{v}} \frac{\partial x^a}{\partial \sigma^u} \frac{\partial x^b}{\partial \sigma^v} g_{ab} \frac{\partial x^{\bar{a}}}{\partial \sigma^{\bar{u}}} \frac{\partial x^{\bar{b}}}{\partial \sigma^{\bar{v}}} g_{\bar{a}\bar{b}}, \\ \epsilon^{u\bar{u}} \frac{\partial x^a}{\partial \sigma^u} \frac{\partial x^{\bar{a}}}{\partial \sigma^{\bar{u}}} &= \frac{1}{2} \epsilon^{u\bar{u}} \frac{\partial x^{a'}}{\partial \sigma^u} \frac{\partial x^{\bar{a}'}}{\partial \sigma^{\bar{u}}} \epsilon_{a'\bar{a}'c} \epsilon^{a\bar{a}c} = n_c \epsilon^{a\bar{a}c}, \\ g g^{c\bar{c}} &= \frac{1}{2} \epsilon^{a\bar{a}c} \epsilon^{b\bar{b}c} g_{ab} g_{\bar{a}\bar{b}}. \end{aligned}$$

(On the role played by surface area in the Ashtekar's formulation of GR, see [50].) We want to construct the quantum area operator $\hat{A}[\Sigma]$, namely, a function of the loop representation operators whose classical limit is $A[\Sigma]$. Following conventional quantum field theoretical techniques, we deal with operator products by defining $\hat{A}[\Sigma]$ as a limit of regularized operators $\hat{A}_\epsilon[\Sigma]$ that do not contain operator products. The difficulty in the present context is to find a regularization that does not break general covariance. This can be achieved by a geometrical regularization [22,10].

Following [23], we begin by constructing a classical regularized expression for the area, namely a one parameter family of classical functions of the loop variables $A_\epsilon[\Sigma]$ which converges to the area as ϵ approaches zero. Consider a small region Σ_ϵ of the surface Σ , whose coordinate area goes to zero with ϵ^2 . For every s in Σ , the smoothness of the classical fields implies that $\tilde{E}^a(s) = \tilde{E}^a(x_I) + O(\epsilon)$, where x_I is an arbitrary fixed point in Σ_ϵ . Also, $U_\alpha(s, t)_A = 1_A^B + O(\epsilon)$ for any $s, t \in \Sigma_I$, and α a (coordinate straight) segment joining s and t . It follows that [because of Eq. (A.1)], to zeroth order in ϵ ,

$$\begin{aligned} \mathcal{T}^{ab}[\alpha_{st}](s, t) &= -\text{Tr}[\tilde{E}^a(s) U_\alpha(s, t) \tilde{E}^b(t) U_\alpha(t, s)] \\ &= 2 \tilde{E}^{a\bar{i}}(x_I) \tilde{E}^{\bar{i}b}(x_I). \end{aligned} \quad (6.4)$$

Using this, we can write

$$\begin{aligned} \epsilon^4 \tilde{E}^{a\bar{i}}(x_I) \tilde{E}^{\bar{i}b}(x_I) &= \frac{1}{2} \int_{\Sigma_\epsilon} d^2 \sigma n_a(\sigma) \int_{\Sigma_\epsilon} d^2 \tau n_b(\tau) \\ &\quad \times \mathcal{T}^{ab}[\alpha_{\sigma\tau}](\sigma, \tau) + O(\epsilon), \end{aligned} \quad (6.5)$$

where $\alpha_{\sigma\tau}$ is, say, a (coordinate) circular loop with the two points σ and τ on antipodal points. Next, consider the area of the full surface Σ . By the very definition of Riemann integral, Eq. (6.3) can be written as

$$\begin{aligned} A[\Sigma] &= \int_\Sigma d^2 \sigma \sqrt{n_a n_b \tilde{E}^{a\bar{i}} \tilde{E}^{b\bar{i}}} \\ &= \lim_{\substack{N \rightarrow \infty \\ \epsilon \rightarrow 0}} \sum_{I_\epsilon} \epsilon^2 \sqrt{n_a(x_I) n_b(x_I) \tilde{E}^{a\bar{i}}(x_I) \tilde{E}^{b\bar{i}}(x_I)} \end{aligned} \quad (6.6)$$

where, following Riemann, we have partitioned the surface Σ in N small surfaces Σ_{I_ϵ} of coordinate area ϵ^2 and x_I is an arbitrary point in Σ_{I_ϵ} . The convergence of the limit to the integral, and its independence from the details of the construction, are assured by the Riemann theorem for all bounded smooth fields. Inserting Eq. (6.5) in Eq. (6.6), we obtain the desired regularized expression for the classical area, suitable to be promoted to a quantum loop operator

$$A[\Sigma] = \lim_{\epsilon \rightarrow 0} A_\epsilon[\Sigma], \quad (6.7)$$

$$A_\epsilon[\Sigma] = \sum_{I_\epsilon} \sqrt{A_{I_\epsilon}^2}, \quad (6.8)$$

$$A_{I_\epsilon}^2 = \frac{1}{2} \int_{\Sigma_{I_\epsilon} \otimes \Sigma_{I_\epsilon}} d^2 \sigma d^2 \tau n_a(\sigma) n_b(\tau) \mathcal{T}^{ab}[\alpha_{\sigma\tau}](\sigma, \tau). \quad (6.9)$$

Notice that the powers of the regulator ϵ in Eq. (6.5) and (6.6) combine nicely, so that ϵ appears in Eq. (6.7) only in the integration domains.

We are now ready to define the area operator

$$\hat{A}[\Sigma] = \lim_{\epsilon \rightarrow 0} \hat{A}_\epsilon[\Sigma], \quad (6.10)$$

$$A_\epsilon[\Sigma] = \sum_{I_\epsilon} \sqrt{\hat{A}_{I_\epsilon}^2}, \quad (6.11)$$

$$\hat{A}_{I_\epsilon}^2 = \frac{1}{2} \int_{\Sigma_{I_\epsilon} \otimes \Sigma_{I_\epsilon}} d^2 \sigma d^2 \tau n_a(\sigma) n_b(\tau) \hat{\mathcal{T}}^{ab}[\alpha_{\sigma\tau}](\sigma, \tau). \quad (6.12)$$

The meaning of the limit in Eq. (6.10) needs to be specified. The specification of the topology in which the limit is taken is an integral part of the definition of the operator. As it is usual for limits involved in the regularization of quantum field theoretical operators, the limit cannot be taken in the

Hilbert space topology where, in general, it does not exist. The limit must be taken in a topology that “remembers” the topology in which the corresponding classical limit (6.7) is taken. This is easy to do in the present context. We say that a sequence of (multi) loops α_ϵ converges to α if α_ϵ converges pointwise to α ; we say that a sequence of quantum states $\langle \alpha_\epsilon |$ converges to the state $\langle \alpha |$ if $\alpha_\epsilon \rightarrow \alpha$ for at least one $\alpha_\epsilon \in \langle \alpha_\epsilon |$ ($\forall \epsilon$) and one $\alpha \in \langle \alpha |$. This definition extends immediately to general states $\langle \Phi |$ by linearity, and defines a topology on the state space, and the corresponding operator topology: $\hat{O}_\epsilon \rightarrow \hat{O}$ iff $\langle \Phi | \hat{O}_\epsilon \rightarrow \langle \Phi | \hat{O}, \forall \langle \Phi |$. Notice that the above is equivalent to say that $\langle \Phi_\epsilon |$ converges to $\langle \Phi |$ if $\mathcal{T}[\Phi_\epsilon]$ converges pointwise to $\mathcal{T}[\Phi]$, which is the topology implicitly used in [15] to regularize the area operator.

An important consequence of the use of this topology is the following. Let $\langle \Phi_\epsilon |$ converge to $\langle \Phi |$. Then the graphs Γ_{Φ_ϵ} converge to Γ_Φ in the topology of M . In other words, given a δ neighborhood of Γ_Φ , there exists an ϵ such that Γ_{Φ_ϵ} is included in the δ neighborhood for all $\epsilon' < \epsilon$. Visually, we can imagine that the ribbon nets R_{Φ_ϵ} “merge” into the ribbon net Γ_Φ^{ex} as ϵ approaches zero. In addition, the representations P_{Φ_ϵ} go to P_{Φ_ϵ} , up to equivalence. This fact allows us to separate the study of a limit in two steps. First, we study of the graph of the limit state. In this process, the representations P_{Φ_ϵ} are merged into the ribbon net R of the limit state. Second, we can use recoupling theory on R , in order to express the limit representation in terms of the spin network basis.

We now study the action of the area operator $\hat{A}[\Sigma]$ given in Eq. (6.10) on a spin network state $\langle S |$. Namely, we compute $\langle S | \hat{A}[\Sigma]$. Let $S \cap \Sigma$ be the set of the points i in the intersection of Γ_S and Σ . In other words, we label by an index i the points where the spin network graph Γ_S and the surface Σ intersect. Generically $S \cap \Sigma$ is numerable, and does not include vertices of S . Here we disregard spin networks that have a vertex lying on Σ or a continuous number of intersection points with Σ . It was pointed out by A. Ashtekar that spin networks with a vertex *and* one -or more- of its adjacent edges lying on Σ are eigenstates of the area with eigenvalues that are not included in the spectrum of the op-

erator computed in [23] and derived again below. Therefore the spectrum of the area given in [23] is not complete. The physical relevance of these “degenerate” cases is unclear to us.⁶

For small enough ϵ , each intersection i will lie inside a distinct Σ_{I_ϵ} surface.⁷ Let us call Σ_{i_ϵ} the surface containing the intersection i (at every fixed ϵ), and e_i the edge through the intersection i . Notice that $\langle S | \hat{A}_{\Sigma_{i_\epsilon}}^2$ vanishes for all surfaces I_ϵ except the ones containing intersections. Thus the sum over surfaces Σ_{I_ϵ} reduces to a sum over intersections. Bringing the limit inside the sum and the square root, we can write

$$\langle S | \hat{A}[\Sigma] = \sum_{i \in \{S \cap \Sigma\}} \langle S | \sqrt{\hat{A}_i^2}, \quad (6.13)$$

$$\hat{A}_i^2 = \lim_{\epsilon \rightarrow 0} \hat{A}_{i_\epsilon}^2. \quad (6.14)$$

For finite ϵ , the state $\langle S | \hat{A}_{i_\epsilon}^2$ has support on the union of the graphs of S and the graph of the loop $\alpha_{\sigma\tau}$ in the argument of the operator (6.12). But the last converges to a point on Γ_S as ϵ goes to zero. Therefore,

$$\lim_{\epsilon \rightarrow 0} \Gamma_{\langle S | \hat{A}_{i_\epsilon}^2} = \Gamma_S. \quad (6.15)$$

The operator $\hat{A}[\Sigma]$ does not affect the graph of $\langle S |$. Next, we have to compute the planar representation of $\Gamma_{\langle S | \hat{A}[\Sigma]}$, which is a tangle on $R_{\langle S | \hat{A}[\Sigma]}$, namely a tangle on R_S . By Eq. (6.13), this is given by a sum of terms, one for each $i \in \{S \cap \Sigma\}$. Consider one of these terms. By definition of the \hat{T} loop operators and of the grasp operation (Sec. III), this is obtained by inserting two trivalent intersections on the spin network edge e_i (inside its ribbon), connected by a new edge of color 2. This is because the circle $\Gamma_{\alpha_{\sigma\tau}}$ has converged to a point on e_i ; in turn, this point is then expanded inside the ribbon as a degenerate loop following back and forward a segment connecting the two intersections. By indicating the representation of the spin network simply by means of its e_i edge, we thus have

$$\begin{aligned} \langle |^{p_e} | \hat{A}_{i_\epsilon}^2 &= \frac{1}{2} \int_{\Sigma_{i_\epsilon} \otimes \Sigma_{i_\epsilon}} d^2\sigma d^2\tau n_a(\sigma) n_b(\tau) \langle |^{p_e} | \hat{T}^{ab}[\alpha_{\sigma\tau}](\sigma, \tau) \\ &= -\frac{l_0^4}{2} \int_{\Sigma_{i_\epsilon} \otimes \Sigma_{i_\epsilon}} d^2\sigma d^2\tau n_a(\sigma) \Delta^a[\beta_e, \sigma] n_b(\tau) \Delta^b[\beta_e, \tau] p_e^2 \left\langle \begin{array}{c} p_e \\ p_e \\ p_e \end{array} \right\rangle^2, \end{aligned} \quad (6.16)$$

where we have already taken the limit (inside the integral) in the state enclosed in the brackets $\langle |$. Notice that this does not

⁶Note added. The complete spectrum of the area has been obtained in the meanwhile in [16], and then reobtained in [51] using the methods developed in this paper.

⁷The (perhaps caviling) issue that an intersection may fall on the *boundary* between two I_ϵ surfaces has been raised. This eventuality, however, does not generate difficulties for the following reason. The integrals we are using are not Lebesgue integrals, because, due to the presence of the δ 's, regions of zero measure of the integration domain cannot be neglected — nor doubly counted. Therefore in selecting the partition of Σ in the I_ϵ surfaces one must include each boundary in one and only one of the two surfaces (which are therefore partially open and partially closed). Boundary points are then normal points that fall inside one and only one integration domain.

depend on the integration variables anymore, because the loop it contains does not represent the grasped loop for a finite ϵ , but the a ribbon expansion of the limit state. Notice also that the two integrals are independent, and equal. Thus, we can write

$$\langle |^{p_e} | \hat{A}_i^2 = -\frac{l_0^4}{2} \left(\int_{\Sigma_{i_\epsilon}} d^2\sigma n_a(\sigma) \Delta^a[\beta_e, \sigma] \right)^2 p_e^2 \left\langle \begin{array}{c} p_e \\ \text{---} \\ p_e \\ \text{---} \\ p_e \end{array} \right\rangle^2. \tag{6.17}$$

The parenthesis is easy to compute. Using Eq. (2.23), it becomes the analytic form of the intersection number between the edge and the surface

$$\int_{\Sigma_{i_\epsilon}} d^2\sigma n_a(\sigma) \Delta^a[\beta_e, \sigma] = \int_{\Sigma_{i_\epsilon}} d^2\sigma n_a(\sigma) \int_{\beta_e} d\tau \dot{\beta}_e^a(\tau) \delta^3[\beta_e(\tau), s] = \pm 1, \tag{6.18}$$

where the sign, which depends on the relative orientation of the loop and the surface, becomes then irrelevant because of the square. Thus

$$\langle |^{p_e} | \hat{A}_i^2 = -\frac{l_0^4}{2} p_e^2 \left\langle \begin{array}{c} p_e \\ \text{---} \\ p_e \\ \text{---} \\ p_e \end{array} \right\rangle^2, \tag{6.19}$$

where we have trivially taken the limit (6.14), since there is no residual dependence on ϵ . We have now to express the tangle inside the bracket in terms of (an edge of) a spin network state. But tangles inside ribbons satisfy recoupling theory, and we can therefore use the formula (E.8) in the Appendix, obtaining

$$\begin{aligned} \langle |^{p_e} | \hat{A}_i^2 &= -l_0^4 p_e^2 \frac{\theta(p_e, p_e, 2)}{2\Delta_{p_e}} \langle |^{p_e} | = l_0^4 \frac{p_e(p_e + 2)}{4} \langle |^{p_e} | \\ &= l_0^4 \frac{p_e}{2} \left(\frac{p_e}{2} + 1 \right) \langle |^{p_e} |. \end{aligned}$$

The square root in Eq. (6.13) is now easy to take because the operator \hat{A}_i^2 is diagonal

$$\langle |^{p_e} | \hat{A}_i = \langle |^{p_e} | \sqrt{\hat{A}_i^2} = \sqrt{l_0^4 \frac{p_e}{2} \left(\frac{p_e}{2} + 1 \right)} \langle |^{p_e} |. \tag{6.20}$$

Inserting in the sum (6.13), and shifting from color to spin notation, we obtain the final result

$$\langle S | \hat{A}[\Sigma] = \left(l_0^2 \sum_{i \in \{S \cap \Sigma\}} \sqrt{j_i(j_i + 1)} \right) \langle S |, \tag{6.21}$$

where j_i is the spin of the edge crossing Σ in i . This result shows that the spin network states (with a finite number of intersection points with the surface and no vertices on the surface) are eigenstates of the area operator. The corresponding spectrum is labeled by multiplets $\vec{j} = (j_1, \dots, j_n)$ of positive half integers, with arbitrary n , and given by

$$A_{\vec{j}}[\Sigma] = l_0^2 \sum_i \sqrt{j_i(j_i + 1)}. \tag{6.22}$$

The spectral values of the degenerate cases in which $\Gamma_S \cap \Sigma$ includes vertices or a continuous number of points, and a discussion on the relevance of these cases, will be given elsewhere.

VII. THE VOLUME OPERATOR

A. The volume in terms of loop variables

Consider a three-dimensional region \mathcal{R} . The volume of \mathcal{R} is given by

$$\begin{aligned} V[\mathcal{R}] &= \int_{\mathcal{R}} d^3x \sqrt{\det g} \\ &= \int_{\mathcal{R}} d^3x \sqrt{\frac{1}{3!} |\epsilon_{abc} \epsilon_{ijk} \tilde{E}^{ai} \tilde{E}^{bj} \tilde{E}^{ck}|}, \end{aligned} \tag{7.1}$$

In order to construct a regularized form of this expression, consider the three index (three hands) loop variable

$$\begin{aligned} \mathcal{T}^{abc}[\alpha](s, t, r) &= -\text{Tr}[\tilde{E}^a(s) U_\alpha(s, t) \tilde{E}^b(t) \\ &\quad \times U_\alpha(t, r) \tilde{E}^c(r) U_\alpha(r, s)]. \end{aligned} \tag{7.2}$$

Because of Eq. (A2), in the limit of the loop $[\alpha]$ shrinking to a point x we have

$$\mathcal{T}^{abc}[\alpha](s, t, r) \rightarrow 2 \epsilon_{ijk} \tilde{E}^{ai} \tilde{E}^{bj} \tilde{E}^{ck} = 2 \epsilon^{abc} \det(\tilde{E}). \tag{7.3}$$

Following [23], fix an arbitrary chart of M , and consider a small cubic region \mathcal{R}_l of coordinate volume ϵ^3 . Let x_l be an arbitrary but fixed point in \mathcal{R}_l . Since classical fields are smooth we have $\tilde{E}(s) = \tilde{E}(x_l) + O(\epsilon)$ for every $s \in \mathcal{R}_l$, and $U_\alpha(s, t)_A^B = 1_A^B + O(\epsilon)$ for any $s, t \in \mathcal{R}_l$ and straight segment α joining s and t . Consider the quantity

$$\begin{aligned} W_l &= \frac{1}{16 \times 3! \epsilon^6} \int_{\partial \mathcal{R}_l} d^2\sigma \int_{\partial \mathcal{R}_l} d^2\tau \int_{\partial \mathcal{R}_l} d^2\rho \\ &\quad \times |n_a(\sigma) n_b(\tau) n_c(\rho) \mathcal{T}^{abc}[\alpha_{\sigma\tau\rho}](\sigma, \tau, \rho)|, \end{aligned} \tag{7.4}$$

where $\alpha_{\sigma\tau\rho}$ is a triangular loop joining the points σ , τ , and ρ . Because of Eq. (7.3), we have, to lowest order in ϵ

$$\begin{aligned}
W_I &= \frac{1}{8 \times 3! \epsilon^6} |\det(\tilde{E}(x_I))| \int_{\partial \mathcal{R}_I} d^2 \sigma \int_{\partial \mathcal{R}_I} d^2 \tau \int_{\partial \mathcal{R}_I} d^2 \rho \\
&\quad \times |n_a(\sigma) n_b(\tau) n_c(\rho) \epsilon^{abc}| \\
&= |\det(\tilde{E}(x_I))|. \tag{7.5}
\end{aligned}$$

Thus W_I is a nonlocal quantity that approximates $\det g(x_I)$ for small ϵ . Using the Riemann theorem as in the case of the area, we can then write the volume $V[\mathcal{R}]$ of the region \mathcal{R} as follows. For every ϵ , we partition of \mathcal{R} in cubes \mathcal{R}_{I_ϵ} of coordinate volume ϵ^3 . Then

$$V[\mathcal{R}] = \lim_{\epsilon \rightarrow 0} V_\epsilon[\mathcal{R}]; \tag{7.6}$$

$$V_\epsilon[\mathcal{R}] = \sum_{I_\epsilon} \epsilon^3 W_{I_\epsilon}^{1/2}. \tag{7.7}$$

B. Quantum volume operator

We have then immediately a definition of the quantum volume operator [23]

$$\hat{V}[\mathcal{R}] = \lim_{\epsilon \rightarrow 0} \hat{V}_\epsilon[\mathcal{R}]; \tag{7.8}$$

$$\hat{V}_\epsilon[\mathcal{R}] = \sum_{I_\epsilon} \epsilon^3 \hat{W}_{I_\epsilon}^{1/2}; \tag{7.9}$$

$$\begin{aligned}
\hat{W}_{I_\epsilon} &= \frac{1}{16 \times 3! \epsilon^6} \int_{\partial \mathcal{R}_I} d^2 \sigma \int_{\partial \mathcal{R}_I} d^2 \tau \int_{\partial \mathcal{R}_I} \\
&\quad \times d^2 \rho |n_a(\sigma) n_b(\tau) n_c(\rho) \hat{\mathcal{T}}^{abc}[\alpha_{\sigma\tau\rho}](\sigma, \tau, \rho)|. \tag{7.10}
\end{aligned}$$

Notice the crucial cancellation of the ϵ^6 factor. We refer to the previous section on the area operator for the discussion on the meaning of the limit and the split of the action of the operator in the computation of the graph and the representation. We will discuss the meaning of the square root later. For alternative definitions of the volume operators, and a discussion on the relation between these, see [24,36] and [17].

Let us now begin to compute the action of this operator on a spin network state. The three surface integrals on the surface of the cube and the line integrals along the loops combine—as in the case of the area—to give three intersection numbers, which select three intersection points between the spin network and the boundary of the cube. In these three points, which we denote as r , s , and t , the loop $\alpha_{\sigma\tau\rho}$ of the operator grasps the spin network.

Notice that the integration domain of the (three) surface integrals is a six-dimensional space—the space of the pos-

sible positions of three points on the surface of a cube. Let us denote this integration domain as D^6 . The absolute value in Eq. (7.10) plays a crucial role here: contributions from different points of D^6 have to be taken in their absolute value, while contributions from the same point of D^6 have to be summed algebraically before taking the absolute value. The position of each hand of the operator is integrated over the surface, and therefore each hand grasps each of the three points r , s , and t , producing 3^3 distinct terms. However, because of the absolute value, a term in which two hands grasp the same point, say r , vanishes. This happens because the result of the grasp is symmetric, but the operator is anti-symmetric, in the two hands — as follows from the antisymmetry of the trace of three sigma matrices. Thus, only terms in which each hand grasps a distinct point give nonvanishing contributions. For each triple of points of intersection between spin network and cube's surface r , s and t , there are $3!$ ways in which the three hands can grasp the three points. These $3!$ terms have alternating signs because of the anti-symmetry of the operator, but the absolute value prevents the sum from vanishing, and yields the same contribution for each of the $3!$ terms.

If there are only two intersection points between the boundary of the cube and the spin network, then there are always two hands grasping in the same point; contributions have to be summed before taking the absolute value, and thus they cancel. Thus the sum in Eq. (7.9) reduces to a sum over the cubes I_ϵ whose boundary has at least three distinct intersections with the spin network, and the surface integration reduces to a sum over the triple graspings in *distinct* points. For ϵ small enough, the only cubes whose surface has at least three intersections with the spin network are the cubes containing a vertex i of the spin network. Therefore, the sum over cubes reduces to a sum over the vertices $i \in \{S \cap \mathcal{R}\}$ of the spin network, contained inside \mathcal{R} . Let us denote by I_{i_ϵ} the cube containing the vertex i . We then have

$$\begin{aligned}
\langle S | \hat{V}[\mathcal{R}] &= \lim_{\epsilon \rightarrow 0} \sum_{i \in \{S \cap \mathcal{V}\}} \epsilon^3 \langle S | \sqrt{|\hat{W}_{I_{i_\epsilon}}|}, \\
\langle S | \hat{W}_{I_{i_\epsilon}} &= \frac{i l_0^6}{16 \times 3! \epsilon^6} \sum_{s,t,r} \langle S \tilde{\#}_{s,t,r} \alpha_{s,t,r} |, \tag{7.11}
\end{aligned}$$

where s, t , and r are three *distinct* intersections between the spin network and the boundary of the box, and we have indicated by $\langle S \tilde{\#}_{s,t,r} \alpha_{s,t,r} |$ the result of the triple grasp of the three hands operator with loop $\alpha_{s,t,r}$ on S .

Let us compute one of the terms above, corresponding to a given triple of grasps, over an n -valent intersections. First of all, in the limit $\epsilon \rightarrow 0$ the operator does not change the graph of the quantum state, for the same reason the area operator does not. Thus the computation reduces to a combinatorial computation of the action of the operator on the representation of the planar state, involving recoupling theory.

Let us represent a spin network state simply by means of the portion of its virtual net containing the vertex on which the operator is acting. We have

Thus $W_{[012]}^{(3)}$ is determined by the Wigner $9J$ symbol (the evaluation of the hexagonal net) as

$$W_{[012]}^{(3)} = \frac{P_0 P_1 P_2 \begin{Bmatrix} P_0 & P_1 & P_2 \\ P_0 & P_1 & P_2 \\ 2 & 2 & 2 \end{Bmatrix}}{\theta(P_0, P_1, P_2)}. \quad (7.18)$$

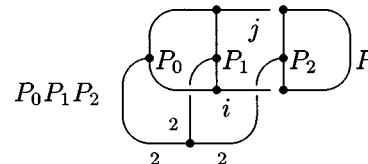
But the hexagonal net (in the case of $A = \pm 1$) it is antisymmetric for the exchange of two columns or of two rows. Therefore the matrix W^3 vanishes, and the trivalent vertices give no contribution to the volume. We have rederived the result that the volume of a three-valent vertex is zero, first obtained by Loll [24].

D. Four-valent vertices

Next, we study the $n = 4$ case:

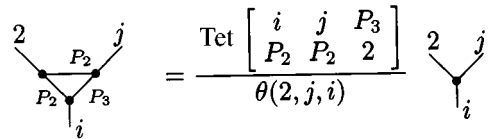
$$\hat{W}_{[012]}^{(4)} \begin{array}{c} P_1 \\ \diagup \\ i \\ \diagdown \\ P_0 \end{array} \begin{array}{c} P_2 \\ \diagdown \\ i \\ \diagup \\ P_3 \end{array} = \sum_j W_{[012]i}^{(4)j} \begin{array}{c} P_1 \\ \diagup \\ j \\ \diagdown \\ P_0 \end{array} \begin{array}{c} P_2 \\ \diagdown \\ j \\ \diagup \\ P_3 \end{array}. \quad (7.19)$$

Using the same technique of the three-valent node we can compute the matrix $W_{[012]i}^{(4)j}$ for a four-valent node as follows:



$$= \sum_k W_{[012]i}^{(4)k} \delta_k^j \frac{\theta(P_0, P_1, j)\theta(P_2, P_3, j)}{\Delta_j}. \quad (7.20)$$

Using the relation



$$= \frac{\text{Tet} \begin{bmatrix} i & j & P_3 \\ P_2 & P_2 & 2 \end{bmatrix}}{\theta(2, j, i)} \begin{array}{c} 2 \\ \diagup \\ j \\ \diagdown \\ i \end{array}, \quad (7.21)$$

we obtain

$$W_{[012]i}^{(4)j} = \frac{P_0 P_1 P_2 \begin{Bmatrix} P_0 & P_1 & j \\ P_0 & P_1 & i \\ 2 & 2 & 2 \end{Bmatrix} \text{Tet} \begin{bmatrix} i & j & P_3 \\ P_2 & P_2 & 2 \end{bmatrix}}{\theta(2, j, i) \theta(P_0, P_1, j) \theta(P_2, P_3, j)}. \quad (7.22)$$

We now prove that the matrix $i \cdot W_{[012]i}^{(4)j}$ is diagonalizable with real eigenvalues and, as a consequence, that its absolute values are well defined. To this aim, let us define the notation

$$A_i^j = \frac{P_0 P_1 P_2 \begin{Bmatrix} P_0 & P_1 & j \\ P_0 & P_1 & i \\ 2 & 2 & 2 \end{Bmatrix} \text{Tet} \begin{bmatrix} i & j & P_3 \\ P_2 & P_2 & 2 \end{bmatrix}}{\theta(2, j, i)}, \quad (7.23)$$

$$M(i) = \sqrt{\frac{\Delta_i}{\theta(P_0, P_1, i) \theta(P_2, P_3, i)}}, \quad (7.24)$$

$$\tilde{W}_i^j = M(i)M(j)A_i^j, \quad (7.25)$$

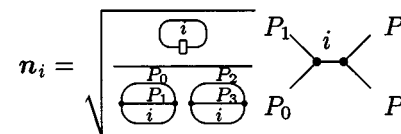
$$S_i^j = \delta_i^j M(i). \quad (7.26)$$

The matrix S_i^j can be consider as a change of basis in the space of the four-valent vertices and the matrix $i \cdot W_{[012]i}^{(4)j}$ can be rewritten as

$$iW_{[012]i}^{(4)j} = (S^{-1})_i^k \cdot (i\tilde{W}_k^l) \cdot S_l^j, \quad (7.27)$$

where, because of the antisymmetry properties of the $9J$ symbol under exchange of two rows and the symmetry prop-

erty of the Tet symbol,⁸ the matrix \tilde{W}_k^l is antisymmetric. We have shown that in the basis



$$\mathbf{n}_i = \sqrt{\frac{\Delta_i}{\theta(P_0, P_1, i) \theta(P_2, P_3, i)}} \begin{array}{c} i \\ \diagup \\ j \\ \diagdown \\ P_0 \end{array} \begin{array}{c} P_2 \\ \diagdown \\ i \\ \diagup \\ P_3 \end{array} \quad (7.28)$$

the action, Eq. (7.19), of the operator $\hat{W}_{[012]}^{(4)}$ is given by

$$\hat{W}_{[012]}^{(4)} \mathbf{n}_i = \sum_j \tilde{W}_{[012]i}^{(4)j} \mathbf{n}_j, \quad (7.29)$$

where $\tilde{W}_{[012]i}^{(4)j}$ a real antisymmetric matrix. Moreover, from the admissibility condition for the three-valent node of Eq. (7.21), we see that \tilde{W}_k^l vanishes unless $k=l$ or $k=l \pm 2$. Thus, we have shown that the operator $i\hat{W}_{[012]}^{(4)}$ may be represented by a purely imaginary antisymmetric matrix $i\tilde{W}_k^l$ with nonvanishing matrix elements only for $k=l \pm 2$. Such matrix is diagonalizable and has real eigenvalues.

⁸For a discussion of the symmetry properties of the $9J$ symbol and related quantities, see for instance [52].

In this way we can bring all three grasps to the edge P_0 . The final step is just given by recognizing that we have Tet structure on the edge P_0 .

Let us begin by applying move 1 to the node r . We obtain

$$(7.35)$$

Then, using move 2 we can move the $(i_r, k_r, 2)$ node to the left of the node (i_{r-1}, P_{r-1}, i_t) :

$$(7.36)$$

We repeat move 2 until the first node with the 2 edge is coupled to the P_0 edge. In this way, after a finite number of moves 2, we have transformed the original network to

$$(7.37)$$

Before repeating this procedure for each of the three grasps, it is convenient to rename the colors k_a of the virtual edges as \bar{k}_a (and to replace the remaining i_a by k_a as well; this can be done by inserting a sum over a \bar{k}_a multiplied by a $\delta_{i_a}^{\bar{k}_a}$).

Repeating the sequence of moves for the two grasps over the edges r and s , we transform the grasped vertex to the final form

$$(7.38)$$

This it is equal to the original n -valent vertex with the i_a replaced by k_a and multiplied by $\text{Tet}[k_1, \bar{k}_1, \bar{k}_1; 2, 2, 2]$ [see Eq. (E9)]. Bringing all together, we have shown that the action of the volume operator is described by the sum (7.15) extended over all vertices of the spin network, where the explicit form for the recoupling matrix (7.13) is given by

$$\begin{aligned}
 W_{[rst]i_2 \dots i_{n-2}}^{(n) k_2 \dots k_{n-2}}(P_0, \dots, P_{n-1}) &= \sum_{\bar{k}_1, \dots, \bar{k}_{n-2}} \sum_{\tilde{k}_1, \dots, \tilde{k}_{n-2}} P_t P_r P_s \cdot \frac{\text{Tet} \begin{bmatrix} \bar{k}_1 & \tilde{k}_1 & k_1 \\ 2 & 2 & 2 \end{bmatrix}}{\Delta_{P_0}} \\
 &\times \left[\prod_{a=r+1}^{n-2} \delta_{i_a}^{\bar{k}_a} \right] \cdot M \begin{bmatrix} i_{r+1} & i_r & \bar{k}_r \\ 2 & r & P_r \end{bmatrix} \cdot \left[\prod_{a=1}^{r-1} \begin{bmatrix} \bar{k}_{a+1} & 2 & \bar{k}_a \\ i_a & P_a & i_{a+1} \end{bmatrix} \right] \\
 &\times \left[\prod_{b=t+1}^{n-2} \delta_{i_b}^{\tilde{k}_b} \right] \cdot M \begin{bmatrix} \bar{k}_{r+1} & \bar{k}_r & \tilde{k}_r \\ 2 & t & P_t \end{bmatrix} \cdot \left[\prod_{b=1}^{t-1} \begin{bmatrix} \tilde{k}_{b+1} & 2 & \tilde{k}_b \\ \bar{k}_b & P_a & \bar{k}_{b+1} \end{bmatrix} \right] \\
 &\times \left[\prod_{c=s+1}^{n-2} \delta_{i_c}^{k_c} \right] \cdot M \begin{bmatrix} \tilde{k}_{s+1} & \tilde{k}_s & k_s \\ 2 & s & P_s \end{bmatrix} \cdot \left[\prod_{c=1}^{s-1} \begin{bmatrix} k_{c+1} & 2 & k_c \\ \tilde{k}_c & P_a & \tilde{k}_{c+1} \end{bmatrix} \right]
 \end{aligned} \quad (7.39)$$

and

$$M \begin{bmatrix} i_{r+1} & i_r & k_r \\ 2 & r & P_r \end{bmatrix} = \begin{cases} 1, & r=0; \\ [\lambda_{k_r}^{2i_r}]^{-1} \begin{bmatrix} i_{r+1} & i_r & k_r \\ 2 & P_r & P_r \end{bmatrix}, & 0 < r < n-1; \\ \lambda_{P_{n-1}}^{2P_{n-1}} = -1, & r = n-1, \end{cases} \quad (7.40)$$

where $i_1 = k_1 = P_0$ and $i_{n-1} = k_{n-1} = \bar{k}_{n-1} = \tilde{k}_{n-1} = P_{n-1}$. (We have used the fact that for $A = -1$, $\lambda_a^{2a} = -1$.)

This formula can be specialized to the case of three-vertex ($n=3$) and four-vertex ($n=4$). In the case of three-vertex we have

$$W^{(3)}(P_0, P_1, P_2) = \left| \sum_{k_1} P_0 P_1 P_2 [\lambda_{P_0}^{2k_1}]^{-1} \begin{bmatrix} P_2 & 2 & P_0 \\ \tilde{k}_1 & P_1 & P_2 \end{bmatrix} \begin{bmatrix} P_2 & P_0 & \tilde{k}_1 \\ 2 & P_1 & P_1 \end{bmatrix} \frac{\text{Tet} \begin{bmatrix} P_0 & \tilde{k}_1 & P_0 \\ 2 & 2 & 2 \end{bmatrix}}{\Delta_{P_0}} \right| \quad (7.41)$$

and a direct computation confirms that the volume of any three-vertex is zero. For the case of four-valent vertex, we obtain the formula

$$W_{[013]i}^{(4)k} = \sum_{k_1} P_0 P_1 P_3 (-1) [\lambda_{P_0}^{2\tilde{k}_1}]^{-1} \begin{Bmatrix} i & P_0 & \tilde{k}_1 \\ 2 & P_1 & P_1 \end{Bmatrix} \begin{Bmatrix} P_3 & 2 & k \\ i & P_2 & P_3 \end{Bmatrix} \begin{Bmatrix} k & 2 & P_0 \\ \tilde{k}_1 & P_1 & i \end{Bmatrix} \frac{\text{Tet} \begin{bmatrix} P_0 & \tilde{k}_1 & P_0 \\ 2 & 2 & 2 \end{bmatrix}}{\Delta_{P_0}}$$

and the other three matrix that appear in the definition of the action of the volume operator are easily deduced from the identities (7.30).

F. Summary of the volume's action

Finally, let us summarize the procedure for computing the eigenvalues and eigenvectors of the volume. Consider the spin-network states $\langle S \rangle$ with a fixed graph and a fixed coloring of the real edges, but with arbitrary intersections. The set of these spin networks forms a finite dimensional subspace V of the quantum state space. The subspace V is invariant under the action of the volume operator. We denote the valence of the real vertex i by n_i . Fix a trivalent decomposition of each vertex $i \in \{S \cup \mathcal{R}\}$. Consider all compatible colorings of the virtual edges. For every vertex, the number of the compatible colorings depends on the valence of the vertex, as well as on the coloring of the external edges. Let N_i be the number of compatible colorings of the vertex n_i . The dimension N of the subspace V we are considering is $N = \prod_i N_i$. Our aim is to diagonalize the volume operator in V .

We indicate a basis in V as follows. Given a vertex i with valence n_i , we have previously denoted compatible colorings of the internal edges by (i_2, \dots, i_{n_i-2}) . It is more convenient here to simplify the notation by introducing a single index $K_i = 1, N_i$, which labels all compatible internal colorings of the vertex i .

We now recall the basic expression we have obtained, for the volume, namely, Eq. (7.15),

$$\hat{V}[\mathcal{V}] = I_0^3 \sum_{i \in \{S \cap \mathcal{V}\}} \hat{V}_i, \quad (7.42)$$

$$\hat{V}_i = \sqrt{\sum_{\substack{r=0, \dots, n-3 \\ t=r+1, \dots, n-2 \\ s=t+1, \dots, n-1}} \left| \frac{i}{16} \hat{W}_{[rts]}^{(n_i)} \right|^2},$$

where the first sum is over the vertices and the second sum is over the triples of edges adjacent to the vertex. We have shown that the operators $i \hat{W}_{[rts]}^{(n_i)}$ are diagonalizable matrices with real eigenvalues. These matrices have components

$$\hat{W}_{[rts]K_i}^{(n_i) \tilde{K}_i} = [\text{LHS of Eq. (7.39)}]. \quad (7.43)$$

Since the matrices $i \hat{W}_{[rts]K_i}^{(n_i) \tilde{K}_i}$ are diagonalizable with real eigenvalues, from the spectral theorem we can write them as

$$i \hat{W}_{[rts]}^{(n_i)} = \sum_{\alpha} \alpha \lambda_{[rts]}^{(n_i)} \alpha \hat{P}_{[rts]}^{(i)}, \quad (7.44)$$

where $\alpha \lambda_{[rts]}^{(n_i)}$ are real quantities and the $\alpha \hat{P}_{[rts]}^{(i)}$ are the spectral projectors of the finite dimensional matrix operator $\hat{W}_{[rts]}^{(n_i)}$ acting on the i th vertex's basis.

From Eq. (7.42), we have then

$$\hat{V}_i^2 = \sum_{\substack{r=0, \dots, n_i-3 \\ t=r+1, \dots, n_i-2 \\ s=t+1, \dots, n_i-1}} \sum_{\alpha} \frac{|\lambda_{\alpha}^{[rts]}|}{16} \alpha \hat{P}_{[rts]}^{(n_i)}. \quad (7.45)$$

Being the sum of Hermitian non-negative matrices, \hat{V}_i^2 as well is diagonalizable with real non-negative eigenvalues, which we denote as $\lambda_{\beta_i}^2$, and spectral projectors P_{β_i} :

$$\hat{V}_i^2 = \sum_{\beta_i} \lambda_{\beta_i}^2 \hat{P}_{\beta_i} \quad (7.46)$$

with $\lambda_{\beta_i} \geq 0$. Therefore we have

$$\hat{V}_i = \sum_{\beta_i} \lambda_{\beta_i} \hat{P}_{\beta_i} \quad (7.47)$$

and the volume is given by

$$\hat{V}[\mathcal{V}] = I_0^3 \sum_{i \in \{S \cap \mathcal{V}\}} \sum_{\beta_i} \lambda_{\beta_i} \hat{P}_{\beta_i}. \quad (7.48)$$

Now, the projectors acting on different vertices commute among themselves: $\hat{P}_{\beta_i} \hat{P}_{\beta_j} = \hat{P}_{\beta_j} \hat{P}_{\beta_i}$ if $i \neq j$. Therefore the eigenvectors of \hat{V} are the common eigenvectors of all \hat{V}_i . They are labeled by one β_i for every vertex i , namely by a multi-index $\vec{\beta} = (\beta_1, \dots, \beta_p)$, where p is the number of vertices in the region. The corresponding spectral projectors $\hat{P}_{\vec{\beta}}$ of \hat{V} are the products over the vertices of the spectral projectors of the vertex volume operators \hat{V}_i

$$\hat{P}_{\vec{\beta}} = \prod_i \hat{P}_{\beta_i}. \quad (7.49)$$

It is immediate to conclude that

$$\hat{V} = I_0^3 \sum_{\vec{\beta}} \lambda_{\vec{\beta}} \hat{P}_{\vec{\beta}}, \quad (7.50)$$

where the eigenvalues of the volume are the sums of the eigenvalues of the volume of each intersection:

$$\lambda_{\vec{\beta}} = \sum_i \lambda_{\beta_i}. \quad (7.51)$$

The problem of the determination of the spectrum of the volume is reduced to a well defined calculation of the eigen-

values λ_{β_i} , which depend on the valence and coloring of adjacent vertices of the vertex i . Let us summarize the various steps of this computation. Given an arbitrary real vertex i with coloring of adjacent edges P_0, \dots, P_{n_i-1} : (i) determine the set of the possible colorings of its virtual edges, and label them by an index K_i ; (ii) using Eq. (7.39) compute the matrix elements $\hat{W}_{[rts]K_i}^{(n_i)}$ (iii) for each of this matrices, compute its spectral decomposition, i.e., the eigenvalues ${}^\alpha\lambda_{[rts]}^{(n_i)}$ and the spectral projectors ${}^\alpha\hat{P}_{[rts]}^{(n_i)}$ (iv) compute the matrix \hat{V}_i from Eq. (7.45); (v) compute the eigenvalues of the matrix \hat{V}_i . The square root of these give the λ_{β_i} 's. All these steps can be fully performed using an algebraic manipulation program such as MATHEMATICA. We have written a MATHEMATICA program that performs these calculations, and we will give free access to this program on line. In Appendix F we give the values of the quantities $\lambda_{\beta_i}(P_0, \dots, P_{n_i-1})$ for some four-valent and five-valent vertex, computed using this program.

G. Complex Ashtekar connection

Before closing this section, let us discuss the modifications that are necessary in order to use the complex Ashtekar connection instead of the real one we have used here. On this subject, see also [41]. The difference is simply the appearance of a factor i in the commutator between the connection and the triad. This yields to an extra i in the factor associated to each grasp. This additional imaginary factor destroys the reality of the eigenvalues of area and volume, which is a main result here. Probably this should be taken as an indication that spin networks constructed from the propagator of the *complex* Ashtekar connection are not physical states. We can illustrate this by means of an analogy. Imagine that we study the eigenvalue equation for the momentum operator $i\hbar \partial/\partial x$ in the quantum mechanics of a single particle. Formally, the functions $\psi(x) = \exp\{kx\}$ solve the eigenvalue equation for any real k . However, the corresponding eigenvalues are imaginary — an indication that these states are not physical. Indeed, they are outside the relevant Hilbert space. The physical eigenstates of the momentum are of the form $\psi(x) = \exp\{ikx\}$, with an i , and these are correct (generalized) physical states. Something similar happens here. In fact, one can check that if we insert an i in the exponent of the holonomies, namely, if we replace Eqs. (2.11) and (2.12) by

$$\frac{d}{d\tau} U_\gamma(\tau, \tau_0) + i \frac{d\gamma^a(\tau)}{d\tau} A_a(\gamma(\tau)) U_\gamma(\tau, \tau_0) = 0 \quad (7.52)$$

and

$$U_\gamma(\tau, \tau_0) = \mathcal{P} \exp \left(-i \int_{\tau_0}^{\tau} d\tau \dot{\gamma}^a A_a(\gamma(\tau)) \right) \quad (7.53)$$

(where A_a^i is now the *complex* Ashtekar connection) then the eigenvalues of area and volume result to be real. Using Eq. (7.53) as the definition of the holonomy implies that the spin

network states correspond (in the connection representation) to combination of parallel propagators of i times the Ashtekar connection. These seem therefore to be the correct physical states related to real geometries. However, this strategy (explored in a previous version of this paper) is not viable, at least in this form. The reason is that Eq. (7.53) is not invariant under the internal gauge transformations generated by the Gauss constraint. Perhaps this difficulty can be circumvented by exploiting the complexity of the group and the nontriviality of the reality conditions, but for the moment we have not been able to find a construction viable for the Riemannian Ashtekar connection. We leave this problem to future investigations.

VIII. THE SCALAR PRODUCT

The results above allow us to introduce a scalar product in the loop representation. The original definition of the loop representation of quantum general relativity left the problem of fixing the scalar product undetermined: the scalar product had to be determined by requiring quantum observables to be Hermitian [3]. The problem was complicated by the fact that the loop ‘‘basis’’ is overcomplete. Later, the introduction of the nonovercomplete spin network basis, and the realization that spin network states (with suitable bases chosen on the high-valent vertices) are eigenstates of the geometry, lead to the natural suggestion that spin network states ought to be orthogonal. For no reason, however, these states ought to be orthonormal; namely the norm of the spin network states remained undetermined. The methods introduced in this paper allow us to complete the process, suggest a norm for the spin network states, and thus yield a complete definition for a scalar product $\langle | \rangle$. Here, we define a scalar product $\langle | \rangle$, and motivate the choice. We have no compelling argument for the uniqueness of this scalar product, but we will show that it satisfies all consistency requirements so far considered. Therefore, it is reasonable to take it as a first ansatz.

Let us begin by considering an n -valent vertex. This can be arbitrarily expanded in trivalent vertices. Let i_1, \dots, i_{n-3} be the colors of the internal edges, and let us represent by $|i_1, \dots, i_{n-3}\rangle$ the n -valent vertex expanded in trivalent vertices colored i_1, \dots, i_{n-3} . We would like to determine an orthogonal basis from the quantities $|i_1, \dots, i_{n-3}\rangle$. We have two highly nontrivial requirements. First, that this works independently from the way the n -valent vertex is expanded in trivalent ones. Second, that the volume be Hermitian in this basis. Rather remarkably, we believe, both requirements can be satisfied.

Let us begin by considering a four-valent vertex, for simplicity. There are two ways in which we can expand it in trivalent vertices. Thus we have two distinct bases $|i\rangle$ and $|i'\rangle$ for the four-valent vertices. If we wanted both of them to be orthonormal, the transformation between the two had to be given by a unitary matrix. Now, the transformation matrix between the two bases is provided by the recoupling theorem. The matrix is given by a six- J symbol, seen as a matrix in its two rightmost entries. It is easy to see that this matrix is not unitary. However, we now show that we can rescale the length of the basis vectors $|i\rangle$ in such a way that the transformation matrix becomes unitary (indeed, orthogonal).

Indeed, let

$$\mathbf{n}_j = \sqrt{\frac{\text{Diagram 1}}{\text{Diagram 2}}} \quad (8.1)$$

Diagram 1: A trivalent vertex with edges labeled a, b, c . The a and b edges are connected to a square loop with a j label inside. The c edge is connected to another trivalent vertex with edges labeled d, j, c .

Diagram 2: A trivalent vertex with edges labeled a, b, c . The a and b edges are connected to a square loop with a j label inside. The c edge is connected to another trivalent vertex with edges labeled d, j, c .

$$\tilde{\mathbf{n}}_i = \sqrt{\frac{\text{Diagram 3}}{\text{Diagram 4}}} \quad (8.2)$$

Diagram 3: A trivalent vertex with edges labeled a, b, c . The a and b edges are connected to a square loop with an i label inside. The c edge is connected to another trivalent vertex with edges labeled d, i, c .

Diagram 4: A trivalent vertex with edges labeled a, b, c . The a and b edges are connected to a square loop with an i label inside. The c edge is connected to another trivalent vertex with edges labeled d, i, c .

In this basis, the recoupling theorem becomes

$$\begin{aligned} \mathbf{n}_j &= \sum_i \sqrt{\frac{\text{Diagram 5}}{\text{Diagram 6}}} \left\{ \begin{matrix} a & b & i \\ c & d & j \end{matrix} \right\} \tilde{\mathbf{n}}_i \\ &= \sum_i \sqrt{\frac{\text{Diagram 7}}{\text{Diagram 8}}} \cdot \tilde{\mathbf{n}}_i \\ &= \sum_i U(a, b, c, d)_j^i \tilde{\mathbf{n}}_i. \end{aligned} \quad (8.3)$$

Diagram 5: A trivalent vertex with edges labeled a, b, c . The a and b edges are connected to a square loop with a j label inside. The c edge is connected to another trivalent vertex with edges labeled d, i, c .

Diagram 6: A trivalent vertex with edges labeled a, b, c . The a and b edges are connected to a square loop with a j label inside. The c edge is connected to another trivalent vertex with edges labeled d, i, c .

Diagram 7: A trivalent vertex with edges labeled a, b, c . The a and b edges are connected to a square loop with a j label inside. The c edge is connected to another trivalent vertex with edges labeled d, i, c .

Diagram 8: A trivalent vertex with edges labeled a, b, c . The a and b edges are connected to a square loop with a j label inside. The c edge is connected to another trivalent vertex with edges labeled d, i, c .

We now prove that the matrix $U(a, b, c, d)_j^i$ is real orthogonal. The inverse transformation matrix from the $\tilde{\mathbf{n}}_i$ basis to the \mathbf{n}_j basis is given by the same expression (8.3), with a reordering of the external edges' colorings: i.e.,

$$\tilde{\mathbf{n}}_k = \sum_i U(d, a, b, c)_i^k \mathbf{n}_i. \quad (8.4)$$

Therefore we have the relation

$$\sum_i U(a, b, c, d)_j^i U(d, a, b, c)_i^k = \delta_j^k. \quad (8.5)$$

From direct inspection of Eq. (8.3) it is easy to see that $U(a, b, c, d)_k^i = U(d, a, b, c)_i^k$. As an immediate consequence of Eq. (8.5) we have orthogonality. Looking at Eqs. (E2) and (E4) we can easily compute the sign of the argument of the square root, which is

$$\begin{aligned} \text{sgn}(\sqrt{}) &= \frac{(-1)^i (-1)^j}{(-1)^{(a+b+j)/2 + (c+d+j)/2 + (a+d+i)/2 + (b+c+i)/2}} \\ &= (-1)^{a+b+c+d} = +1. \end{aligned} \quad (8.6)$$

We have thus shown that there exists a basis in which the recoupling theorem yields a unitary transformation. For higher valence vertices, the transformation from one trivalent expansion to another can be obtained by a repeated applications of the recoupling theorem transformation, and therefore by a product of orthogonal matrices. Thus the argument above extends immediately to higher valence.

Now, the normalization we have found is exactly the one in which the volume operator is represented by a real anti-

symmetric matrix, as shown by Eqs. (7.23) and (7.27). Therefore we have found a basis that satisfies all our requirements.

We thus define the normalized spin-network states by the following normalization: given an arbitrary spin-network state $\langle S|$, we label with an index $i \in V$ all the three-valent vertices of the expanded state (virtual and real) and with a index $e \in \mathcal{E}$ all its edges (virtual and real). We denote the color of the edge e by with p_e and the color of the three edges adjacent to the vertex i by $a_i, b_i,$ and c_i . We define the *normalized* spin network state $\langle S|_N$ by

$$\langle S|_N = \sqrt{\prod_{i \in V} \prod_{e \in \mathcal{E}} \frac{\Delta_{p_e}}{\theta(a_i, b_i, c_i)}} \langle S| \quad (8.7)$$

and we define a scalar product on \mathcal{V} by requiring that these states are orthonormal. We have immediately from the discussion above that the definition does not depend on the trivalent expansion chosen, and that the volume and area operators are symmetric with respect to this scalar product.

We think that the scalar product defined in this way is precisely the one defined on the loop representation by the loop transform [3,4] of the Ashtekar-Lewandowski measure [53], namely the conventional Haar measure lattice gauge theory scalar product for each graph. The precise relation is discussed by Reisenberger [33] and in [18]. In turn, we expect that (the norm derived from) the scalar product we have defined is equivalent to the evaluation of the Kauffman bracket of the state, and to the trace of the Temperley-Lieb algebra, discussed in Appendix B.

IX. CONCLUSIONS AND FUTURE DIRECTIONS

We have reviewed the kinematics of the loop representation of quantum gravity, and presented a number of results. We have modified the definition of the theory by inserted a minus sign in the definition of the loop observables. With this convention, the spinor identity is transformed into the binor identity, allowing immediately a local graphical calculus for the grasping operation and the use of recoupling theory. We have shown that the loop states obey the axioms of recoupling theory, and the corresponding graphical formalism provides a powerful tool for computing the action of geometrical operators. We have discussed in detail the way in which recoupling theory can be used in this context.

Using recoupling theory, we have rederived known results on the eigenstates of the area, and the volume of trivalent and four-valent vertices. We have given a general expression for the volume of higher valence vertices. We have proven that the square root in the volume operator is well defined, because the relevant operator is Hermitian. We have defined a scalar product by a suitable normalization of the trivalent spin networks. We have shown that that the scalar product is well defined and independent from the trivalent expansion chosen, and that the volume is symmetric with respect to this scalar product.

Notice that the area and volume operators \hat{A} and \hat{V} do not correspond to physical observables: they are not gauge invariant and do not commute with GR's constraints. The areas and volumes that we routinely measure are associated to spatial regions determined by matter. Indeed, the area and vol-

ume of regions determined by physical matter *are* represented on the phase space of the coupled gravity-matter theory by observables which are gauge invariant (see for instance [54]). However, it was suggested in Ref. [25] that it is reasonable to expect that these physical areas and volumes (of spatial regions determined by matter) be *still* expressed by (operators unitary equivalent to) \hat{A} and \hat{V} . See Refs. [54] and [25] for the details of the argument. If this suggestion is correct, the spectra computed here can be taken as physical predictions on short scale geometry, following from the loop representation of quantum gravity [25]. These predictions are testable in principle, and could perhaps lead to indirect observable consequences.

We consider the following open problems particularly important for the development of the theory.

We have not explored the degenerate cases in the action of the area operator (but see [16,51]).

We believe that the formalism is now well established for a precise discussion of the Hamiltonian and for computing transition amplitudes [26,27].

Can a weave [22] be found for which not just the area but the volume as well approximates smooth geometries? Can a weave related to a four-dimensional geometry [55] be constructed?

A way of implementing the Lorentzian reality conditions is, to our knowledge, still lacking (for an attempt to address this problem, see [39]).

Under the optimistic assumption that the above technical problems could be addressed, a possible first task for the theory could be the following: Compute the clock time evolution of a weave representing a black hole, show that Hawking's radiation [56] is emitted, and determine the final stage of the black hole after evaporation.

Supposing that area and volume eigenvalues computed here describe an actual physical discreteness (in the quantum sense) of Planck scale geometry, could there be any low energy observable consequence of such discreteness?⁹

ACKNOWLEDGMENTS

We thank Mike Reisenberger and Lee Smolin for teaching us the relevance of recoupling theory and of its tangle theoretical version, Roumen Borissov, Simonetta Frittelli, Viqar Husain, Giorgio Immirzi, Luis Lehner, and Renate Loll for a careful reading of the manuscript and many important suggestions, and Seth Major and Abhay Ashtekar for valuable criticisms and insights. One of us (R.D.P.) thanks the members of the Relativity group of Pittsburgh, where this work began, for their warm hospitality, as well as Massimo Pauri and Luca Lusanna for their continuous support and encouragement. This work has been partially supported by the NSF Grant NO. PHY-90-12099 (USA), by the INFN grant "Iniziativa specifica FI-41" (Italy), and by the Human Capital and Mobility Program "Constrained Dynamical Systems" (European Union).

⁹Note added. Two applications of these results have been studied after the appearance of the preprint of this paper: one on black hole's emission spectrum [57], and one on black hole entropy [58].

APPENDIX A: PAULI MATRICES IDENTITIES

Defining $\tau_i = -(i/2) \sigma_i$, where σ_i are the Pauli matrices, we have the identities

$$\text{Tr}[\tau_i \tau_j] = -\frac{1}{2} \delta_{ij}, \quad (\text{A1})$$

$$\text{Tr}[\tau_i \tau_j \tau_k] = -\frac{1}{4} \epsilon_{ijk}, \quad (\text{A2})$$

$$\delta^{ij} \tau_{iA}^B \tau_{jC}^D = -\frac{1}{4} (\delta_A^D \delta_B^C - \epsilon^{BD} \epsilon_{AC}), \quad (\text{A3})$$

$$\delta^{ij} \text{Tr}[A \tau_i] \text{Tr}[B \tau_j] = -\frac{1}{4} \{\text{Tr}[AB] - \text{Tr}[AB^{-1}]\}, \quad (\text{A4})$$

$$A^{-1B}{}_A = \epsilon^{BD} \epsilon_{AC} A^C{}_D, \quad (\text{A5})$$

$$\delta_A^B \delta_D^C = \delta_A^C \delta_D^B + \epsilon^{BC} \epsilon_{AD}, \quad (\text{A6})$$

$$\text{Tr}[A] \text{Tr}[B] = \text{Tr}[AB] + \text{Tr}[AB^{-1}], \quad (\text{A7})$$

where A and B are $\text{SL}(2, C)$ matrices.

APPENDIX B: KAUFFMAN BRACKETS AND TEMPERLEY-LIEB RECOUPLING THEORY

In the context of Knot theory [32], the appearance of recoupling theory is based on the observation that the Kauffman bracket satisfies the properties (and is completely determined by the properties)

$$\langle \text{X} \rangle = A \langle \text{Y} \rangle + A^{-1} \langle \text{Z} \rangle \quad (\text{B1})$$

and

$$\langle \text{O} \cup \mathbf{K} \rangle = d \langle \mathbf{K} \rangle \quad (\text{B2})$$

where $\langle \rangle$ denotes the Kauffman bracket, where $d = -A^2 - A^{-2}$ and \mathbf{K} is any diagram that does not intersect the added loop. These properties of the Kauffman bracket are sufficient to generate the entire formalism of recoupling theory. In particular, they generate a "tangle theoretic" interpretation of the Temperley-Lieb algebra as follows.

A planar tangle is a set of lines on a plane. It is possible to write an arbitrary tangle inside the Kauffman brackets as the sum of nonintersecting tangles by applying Eq. (B1) to all crossings. In [59] it is shown that every planar nonintersecting n tangle with n inputs and n outputs is equivalent to the

product of elementary tangles $\mathbb{1}_n, U_1, \dots, U_{n-1}$, given by

$$\begin{aligned} \mathbb{1}_n &= \text{stack of } n \text{ vertical lines} \\ U_1 &= \text{cup on } n \text{ vertical lines} \\ &\vdots \\ U_{n-1} &= \text{cup on } n \text{ vertical lines} \end{aligned}$$

where the product is interpreted as a stacking of two diagrams. Two such products represent tangles equivalent under the Kauffman brackets if and only they can be transformed into each other by the relations

$$U_i^2 = dU_i, \tag{B3}$$

$$U_i U_{i\pm 1} U_i = U_i, \tag{B4}$$

$$U_i U_j = U_j U_i, |i-j| > 1, \tag{B5}$$

which are at the basis of the Temperley-Lieb algebra. For example, Eq. (B3), means

$$U_i U_i = \text{cup-cup} = \text{cup-cup} = d \mathbb{1}_i. \tag{B6}$$

Given an n tangle x , let \bar{x} denote the standard closure of x , obtained by attaching the k th input to the k th output:

$$x \Rightarrow \bar{x} = \text{closure of } x$$

The Temperley-Lieb algebra T_n is the free additive algebra over $\mathbb{Z}[A, A^{-1}]$ with multiplicative generators $\mathbb{1}_n, U_1, \dots, U_{n-1}$. The trace on the algebra T_n is defined as follows: (i) If x is an n tangle then $\text{tr}(x) = \langle \bar{x} \rangle$ where $\langle \rangle$ denotes the Kauffman brackets, or, which is the same, the recursive evaluation of \bar{x} using Eqs. (B1) and (B2); (ii) $\text{tr}(x+y) = \text{tr}(x) + \text{tr}(y)$.

1. The Jones-Wenzel projector

It can be shown [32] that in the Temperley-Lieb algebra T_n there exist one (and only one) element $\Pi_n \in T_n$ such that $\Pi_n^2 = \Pi_n$ and $\Pi_n U_i = U_i \Pi_n, i = 1, \dots, n-1$. This unique element is called the Jones-Wenzel projector of T_n . Its explicit expression is given by

$$\Pi_n = \frac{\text{cap}}{\text{cup}} = \frac{1}{n!} \sum_p (A^{-3})^{|p|} P_n^{(p)}. \tag{B7}$$

$P(p), p = 1, \dots, n!$ is the n tangle obtained by all possible permutations p in the way the n lines entering e are connected to the n outgoing lines, $P_n^{(p)}$ its a minimal representation of the permutation (p) , and $|p|$ its the parity of the representation. Since any n tangle can be expanded, using

Eq. (B1), in a sum of *nonintersecting* tangles, the expression (B7) is an element of T_n . As an example we give the definition of Π_2 :

$$\begin{aligned} \Pi_2 &= \frac{\text{cap}}{\text{cup}} = \frac{1}{\{2\}!} \left[\left| \begin{array}{c} | \\ | \end{array} \right. + A^{-3} \begin{array}{c} \diagdown \\ \diagup \end{array} \right] \\ &= \frac{1}{1+A^{-4}} \left[\left| \begin{array}{c} | \\ | \end{array} \right. + A^{-4} \left| \begin{array}{c} | \\ | \end{array} \right. + A^{-2} \begin{array}{c} \cup \\ \cup \end{array} \right] \\ &= \left| \begin{array}{c} | \\ | \end{array} \right. + \frac{1}{A^2 + A^{-2}} \begin{array}{c} \cup \\ \cup \end{array} \\ &= \left| \begin{array}{c} | \\ | \end{array} \right. - \frac{1}{d} \begin{array}{c} \cup \\ \cup \end{array} = \mathbb{1}_2 - \frac{1}{d} U_1. \end{aligned}$$

In the $A = -1$ case the projectors reduce to antisymmetrizers.

2. A special sum of tangles: the three-vertex

A special sum of tangles is indicated by a three-vertex. Each line of the vertex is labeled with a positive integer a, b , or c as shown below



and it is assumed that $m = (a+b-c)/2, n = (b+c-a)/2$, and $p = (c+a-b)/2$ are positive integers. This last condition is called the *admissibility condition* for the three-vertex (a,b,c) . A line labeled by a positive integer a is interpreted as the nonintersecting n tangle $\mathbb{1}_a$. The three-vertex is then defined as

$$\text{three-vertex} \stackrel{def}{=} \text{cap} \begin{array}{c} \text{---} a \text{---} \\ \text{---} p \text{---} \\ \text{---} n \text{---} \\ \text{---} b \text{---} \\ \text{---} c \text{---} \end{array} \tag{B8}$$

Here, it is understood that each Temperley-Lieb projector is fully expanded. For instance,

$$\begin{aligned} \text{three-vertex}(1,1,2) &= \text{Y-vertex} - \frac{1}{d} \text{cup} \\ \text{three-vertex}(2,2,2) &= \text{Y-vertex} + \frac{2}{d^2} \text{cup} \\ &= -\frac{1}{d} \left[\text{Y-vertex} + \text{cup} + \text{Y-vertex} \right] \end{aligned}$$

3. Chromatic evaluation

If we join trivalent vertices by their edges, we obtain trivalent networks. Thus, in the present context a trivalent spin network is defined as a trivalent graph with an admissible coloring. Notice that in this context spin networks are not embedded in a three-dimensional space. An edge of color n represents n parallel lines and a Jones-Wenzel projector, and a vertex is understood as completed expanded in terms of nonintersecting tangles, as above. Thus a trivalent spin network determines a closed tangle. We can compute the Kauffman bracket, or the Temperley-Lieb trace, of such a

tangle. This is also called the chromatic evaluation, or network evaluation. The explicit calculation of the trace is generally based on a generalization of the chromatic method of spin-network evaluation [60]. In Ref. [60] this method is used in order to compute the Clebsch-Gordan coefficients for the group $SU(2)$.

Chromatic evaluations of simple networks are given in Appendix E. We refer to [32] for the details of the computations. Here, we perform one such computation explicitly, as an example. Let us consider the spin network formed by two trivalent vertices joined to each other. This is called the θ network. Consider the case with edges of color 2,1,1:

$$\begin{aligned} \textcircled{\frac{1}{1}} &= \textcircled{\frac{1}{2} \frac{2}{1}} = \textcircled{\frac{1}{2} \frac{2}{1}} - \frac{1}{d} \textcircled{\frac{1}{2} \frac{2}{1}} \\ &= d^2 - \frac{1}{d}d = d^2 - 1 = -(A^2 + A^{-2})^2 - 1 \\ &= [3] = \frac{(-1)^{0+1+1}[3]![1]![1]![0]!}{[2]![1]![1]!} \end{aligned} \tag{B9}$$

We have (1) expanded the trivalent vertices explicitly; (2) computed the trace using Eq. (B2); (3) written the expression in terms of quantum integer (E1); (4) compared the result with the general formula of the chromatic evaluation of the θ net (E4). In the $A = -1$ case, the above gives

$$\textcircled{\frac{1}{2} \frac{2}{1}} = 3 \tag{B10}$$

APPENDIX C: PENROSE THEORY OF SPIN NETWORK

In this appendix we discuss the relation between the Penrose theory of spin networks and the Kauffman bracket and Temperley-Lieb recoupling theory. This appendix is based essentially on Penrose’s original formulation [43] and on an article by Kauffman [61]. A basic idea used by Penrose (in his doctoral thesis) is to rewrite any tensor expression in which there are sums of indices in a graphical way [31]. Consider the calculus of spinors. Penrose represents the basic element of spinor calculus as

$$\delta_C^A = \begin{array}{c} \bullet^A \\ | \\ \bullet_C \end{array} \tag{C1a}$$

$$\epsilon_{AC} = \begin{array}{c} \bullet \\ \diagup \quad \diagdown \\ \bullet_A \quad \bullet_C \end{array} \tag{C1b}$$

$$\eta_A = \begin{array}{c} \boxed{\eta} \\ \bullet_A \end{array} \tag{C1c}$$

$$\epsilon^{AC} = \begin{array}{c} \bullet^A \\ \diagdown \quad \diagup \\ \bullet_C \quad \bullet^A \end{array} \tag{C1b}$$

$$\eta^A = \begin{array}{c} \bullet^A \\ \boxed{\eta} \end{array} \tag{C1c}$$

and generally to any tensor object

$$X_{AB}^C = \begin{array}{c} \bullet^C \\ \boxed{X} \\ \bullet_A \quad \bullet_B \end{array} \tag{C1d}$$

This convention provides the possibility of writing the product of any two tensors in a graphical way. For example,

$$\epsilon_{AB} \eta^A \eta^B = \begin{array}{c} \bullet^A \quad \bullet^B \\ \boxed{\eta} \quad \boxed{\eta} \end{array} \tag{C2}$$

$$= -\epsilon_{AD} \epsilon_{BC} \epsilon^{CD} \eta^A \eta^B = - \begin{array}{c} \bullet^A \quad \bullet^B \quad \bullet^C \quad \bullet^D \\ \boxed{\eta} \quad \boxed{\eta} \quad \bullet \quad \bullet \end{array} \tag{C3}$$

$$= -\epsilon_{CD} \delta_A^D \delta_B^C \eta^A \eta^B = - \begin{array}{c} \bullet^C \quad \bullet^D \\ \boxed{\eta} \quad \boxed{\eta} \end{array} \tag{C4}$$

In the light of the example above, Penrose considered a modification of the spinor calculus, which he denoted as binor calculus. The binor calculus is obtained by adding two conventions to the calculus above: (1) Assign a minus sign to each minimum; (2) assign a minus sign to each crossing; (3) maxima and minima are taken with respect to a fixed direction in the plane (this direction is conventionally taken to be the vertical direction on the written page); (4) a segment with transversal intersection with all horizontal direction is taken to be a Kronecker δ . The advantage of these additional rules is that they make the calculus topological invariant, namely one can arbitrarily smoothly deform a graphical expression without changing its meaning.

The other way around, any curve can now be decomposed in a product of δ ’s and ϵ ’s and any two curves that are ambient isotopic, i.e., that can be transformed one in the other by a sequence of Reidemeister moves, represent the tensorial expression as product of ϵ ’s and δ ’s.

A closed loop (with this convention) has value (-2) , because

$$\bigcirc = -\epsilon_{AB} \epsilon^{AB} = -2 \tag{C5}$$

and we have the basic binor identity, which reads

$$\begin{array}{c} \times \\ + \\ | \\ + \\ \smile \end{array} = (-1) \delta_B^C \delta_A^D + \delta_A^C \delta_B^D + (-1) \epsilon_{AB} \epsilon^{CD} = 0 \tag{C6}$$

It is easy to see that these relations are exactly the same as the properties (B1) and (B2) of the Kauffmans brackets with $A = -1$ and $d = -2$. Notice from Eq. (B1) that if $A = -1$ undercrossing and overcrossing are equivalent: indeed they give the same expansion. Clearly in Penrose’s binor calculus there is no meaning of the distinction between over and undercrossing. The theory can then be developed as the recoupling theory of Appendix B with the special value $A = -1$. Thus the $A = -1$ Kauffman bracket of a spin network is the same as the Penrose’s spin network evaluation.

For more detail on the exact relation between *tangle-theoretic* recoupling theory and spin networks see, for example [32,46,61]. An important point that emerges from this brief discussion is the possibility of using a topological invariant calculus for writing generic $SL(2,C)$ invariant tensor expressions. (This was one of the original motivations of Penrose for introducing binors.) It is possible to write any $SL(2,C)$ Mandelstam identities (3.3) in a graphical way and in particular we can express these identities in spin-network-like graphical relations, in which each edge is the antisymmetrization of the holonomies along the edge.

APPENDIX D: GRAPHICAL CALCULUS OF ANGULAR MOMENTUM AND ITS RELATION WITH THE TANGLE-THEORETICAL RECOUPLING THEORY

Finally, the $A = -1$ case of recoupling theory is equivalent to the graphical calculus of the algebra of the $SU(2)$ representations. In the literature there is a great number of results on the Wigner $3nJ$ symbols and a well developed theory of graphical calculus for angular momentum. To our knowledge the most used graphical method of computation in the representation theory of $su(2)$ are the one due to Levinson [62] and developed by Yutsis, Levinson, and Vanagas [63] and the slightly modified version of Brink and Satcheler [52]. We discuss here the connection between the tangle-theoretical recoupling theory (in the case $A = 1$)¹⁰ and the graphical method of Brink and Satcheler [52]. We indicate a diagram in the Brink convention with a subscript B , and the $3nJ$ symbol (in the standard normalization¹¹) with a subscript W . The two methods are identical up to a different normalization of the three-valent vertex and the fact the the orientations of any vertex are explicit denoted with a $+$ for a counter-clockwise orientation and $-$ for a clockwise one. (In this appendix we are imprecise about this overall sign.) Following Kauffman, we have chosen to denote the recoupling matrix of a four-valent node by curly brackets, while curly brackets are used in the angular momentum literature to indicate Wigner's $6J$ symbols, which are the evaluation of the tetragonal net. In other words, the Wigner $3J$ and $6J$ symbol are defined as the evaluation

$$\{a, b, c\}_W = \text{norm} \cdot \theta(a, b, c), \tag{D1}$$

$$\left\{ \begin{matrix} a & b & c \\ d & e & f \end{matrix} \right\}_W = \text{norm} \cdot \text{Tet} \left[\begin{matrix} a & b & c \\ d & e & f \end{matrix} \right], \tag{D2}$$

where the normalization factor ‘‘norm’’ of [52] corresponds to the choice

$$\{a, b, c\}_W = \left(\begin{matrix} a \\ b \\ c \end{matrix} \right)_B = +1 \tag{D3}$$

This is also the standard normalization of the Clebsh-Gordon coefficient that gives the usual normalization of the Wigner $3nJ$ symbol. With this normalization the recoupling theorem [Eq. (E5)] becomes

¹⁰The correspondence between the case $A = -1$ and $A = 1$ and their equivalence is discussed by Penrose in [31].

¹¹We recall the fact that we use color and not spin to denote the $su(2)$ representation associated to an edge. In the angular momentum literature, the spin notation is prevalent. As a consequence, numbers in Brink diagrams, or in $3nJ$ symbols in standard normalization, must be understood as the spin of the edge; or, equivalently, the color divided by two.

$$\left(\begin{matrix} b & & c \\ & j & \\ a & & d \end{matrix} \right)_B = \sum_i \Delta_i \left\{ \begin{matrix} a & b & i \\ c & d & j \end{matrix} \right\}_W \left(\begin{matrix} b & & c \\ & i & \\ a & & d \end{matrix} \right)_B, \tag{D4}$$

where Δ_i is interpreted as the dimension of the representation of spin $i/2$. From Eqs. (D3) and (D4) we have the correspondence between a Brink diagram and one of ours: one has to divide any three-valent node by $\sqrt{\theta(a, b, c)}$. As an example, let us consider the relation between the tetrahedron evaluation (Tet) and the Wigner $6J$ symbol:

$$\left\{ \begin{matrix} A & B & E \\ C & D & F \end{matrix} \right\}_W = \left(\begin{matrix} B & & C \\ & F & \\ A & & D \end{matrix} \right)_B = \frac{\text{Tet} \left[\begin{matrix} A & B & E \\ C & D & F \end{matrix} \right]}{\sqrt{\theta(A, B, F)\theta(C, D, F)\theta(A, D, E)\theta(B, C, E)}} \tag{D5}$$

APPENDIX E: BASIC FORMULAS OF RECOUPLING THEORY

We collect here the basic formulas of recoupling theory in the case $A = -1$ and $d = -2$. Using the ‘‘quantum’’ integer

$$[n] = \frac{A^{2n} - A^{-2n}}{A^2 - A^{-2}} = (-1)^{n-1} \Delta_{n-1} = n, \tag{E1}$$

$$\{n\} = \frac{1 - A^{-4n}}{1 - A^{-4}} = A^{2n-2} [n] = n, \tag{E1}$$

$$\{n\}! = \{1\} \cdot \{2\} \cdot \dots \cdot \{n\} = n!$$

we define (1) the symmetrizer

$$\Delta_n = \left(\begin{matrix} n \\ \square \end{matrix} \right) = (-1)^n [n+1] = (-1)^n (n+1), \tag{E2}$$

(2) the exchange of line in a three-vertex,

$$\left(\begin{matrix} a & & b \\ & c & \\ & & c \end{matrix} \right) = \lambda_c^{ab} \left(\begin{matrix} a & & b \\ & c & \\ & & c \end{matrix} \right), \tag{E3}$$

where $\lambda_c^{ab} = (-1)^{(a+b-c)/2} A^{(a'+b'-c')/2}$, and $x' = x(x+2)$, (3) the θ evaluation

$$\theta(a, b, c) = \frac{a}{\frac{b}{\frac{c}{a}}} = \frac{(-1)^{m+n+p} [m+n+p+1]! [m]! [n]! [p]!}{[a]! [b]! [c]!}, \quad (E4)$$

where $m = (a+b-c)/2$, $n = (b+c-a)/2$, $p = (c+a-b)/2$, (4) the recoupling theorem

$$\begin{matrix} b & & c \\ & \diagdown & / \\ & j & \\ & / & \diagdown \\ a & & d \end{matrix} = \sum_i \left\{ \begin{matrix} a & b & i \\ c & d & j \end{matrix} \right\} \begin{matrix} b & & c \\ & \diagdown & / \\ & i & \\ & / & \diagdown \\ a & & d \end{matrix}, \quad (E5)$$

$$\left\{ \begin{matrix} a & b & i \\ c & d & j \end{matrix} \right\} = \frac{\Delta_i \text{Tet} \begin{bmatrix} a & b & i \\ c & d & j \end{bmatrix}}{\theta(a, d, i) \theta(b, c, i)}, \quad (E6)$$

(5) the tetrahedral net

$$\text{Tet} \begin{bmatrix} A & B & E \\ C & D & F \end{bmatrix} = \frac{\text{Diagram}}{\text{Diagram}} = \frac{\mathcal{I}}{\mathcal{E}} \sum_{m \leq S \leq M} \frac{(-1)^S [S+1]!}{\prod_i [S-a_i]! \prod_j [b_j-S]!}, \quad (E7)$$

where

$$a_1 = \frac{A+D+E}{2}, \quad b_1 = \frac{B+D+E+F}{2},$$

$$a_2 = \frac{B+C+E}{2}, \quad b_2 = \frac{A+C+E+F}{2},$$

$$a_3 = \frac{A+B+F}{2}, \quad b_3 = \frac{A+B+C+D}{2},$$

$$a_4 = \frac{C+D+F}{2},$$

$$m = \max\{a_i\}, \quad M = \min\{b_j\},$$

$$\mathcal{E} = [A]! [B]! [C]! [D]! [E]! [F]!, \quad \mathcal{I} = \prod_{ij} [b_j - a_i]!,$$

and (6) the reduction formula

$$\begin{matrix} & a & \\ & | & \\ b & \circ & c \\ & | & \\ & a & \end{matrix} = \frac{\begin{matrix} a & \\ \frac{b}{\frac{c}{a}} \end{matrix}}{\begin{matrix} a \\ \frac{a}{a} \end{matrix}} \cdot \left| \begin{matrix} a \\ \frac{a}{a} \end{matrix} \right. \quad (E8)$$

$$\begin{matrix} & a & \\ & | & \\ b & \circ & d \\ & | & \\ c & \circ & e \\ & | & \\ & a & \end{matrix} = \frac{\begin{matrix} c & d \\ \frac{f}{\frac{a}{\frac{b}{\frac{d}{e}}}} \end{matrix}}{\begin{matrix} a \\ \frac{a}{a} \end{matrix}} \cdot \left| \begin{matrix} a \\ \frac{a}{a} \end{matrix} \right. \quad (E9)$$

These formulas are sufficient for the computations performed in the paper. For details on their derivation, see [32].

APPENDIX F: SOME VOLUME EIGENVALUES

Finally, we present here some volume eigenvalues of four- and five-valent vertices. Tables I and II give the colors of the external edges, the dimension of the vertex (number of independent compatible colorings), and the eigenvalues. The numbers in parentheses indicate the multiplicity of the eigenvalues.

TABLE I. The eigenvalues of the volume for some four-valent vertices.

P_0	P_1	P_2	P_3	Dim.	$\lambda_{\beta_i} = \lambda_{\beta_i}(P_0, \dots, P_3)$
1	1	1	1	2	$(2) \sqrt{\frac{1}{8}\sqrt{3}}$
2	2	2	2	3	$(1)0, (2) \sqrt{\frac{1}{2}\sqrt{3}}$
3	3	3	3	4	$(2) \sqrt{\frac{3}{8}\sqrt{3}}, (2) \sqrt{\frac{3}{8}\sqrt{35}}$
4	4	4	4	5	$(1)0, (2) \sqrt{\frac{3}{4}\sqrt{22-2\sqrt{57}}}, (2) \sqrt{\frac{3}{4}\sqrt{22+2\sqrt{57}}}$
5	5	5	5	6	$(2) \sqrt{\frac{1}{8}\sqrt{1155}}, (2) \sqrt{\frac{1}{8}\sqrt{2211-96\sqrt{481}}}, (2) \sqrt{\frac{1}{8}\sqrt{2211+96\sqrt{481}}}$
6	6	6	6	7	$(1)0, (2) \sqrt{2\sqrt{3}}, (2) \sqrt{\frac{9}{2}\sqrt{3}}, (2) \sqrt{\frac{1}{2}\sqrt{723}}$
1	1	1	1	2	$(2) \sqrt{\frac{1}{8}\sqrt{3}}$
2	2	1	1	2	$(2) \sqrt{\frac{1}{4}\sqrt{2}}$
3	2	2	1	2	$(2) \sqrt{\frac{1}{4}\sqrt{5}}$
3	3	1	1	2	$(2) \sqrt{\frac{1}{8}\sqrt{15}}$
3	3	3	1	2	$(2) \sqrt{\frac{1}{2}\sqrt{3}}$
4	2	2	2	2	$(2) \sqrt{\frac{1}{2}\sqrt{3}}$
4	3	2	1	2	$(2) \sqrt{\frac{3}{4}}$
4	4	1	1	2	$(2) \sqrt{\frac{1}{4}\sqrt{6}}$
4	4	3	1	2	$(2) \sqrt{\frac{1}{4}\sqrt{21}}$
5	3	2	2	2	$(2) \sqrt{\frac{1}{4}\sqrt{21}}$
5	3	3	1	2	$(2) \sqrt{\frac{3}{8}\sqrt{7}}$
5	4	2	1	2	$(2) \sqrt{\frac{1}{4}\sqrt{14}}$
5	4	4	1	2	$(2) \sqrt{\frac{3}{2}}$
5	5	1	1	2	$(2) \sqrt{\frac{1}{8}\sqrt{35}}$
5	5	3	1	2	$(2) \sqrt{\sqrt{2}}$
5	5	5	1	2	$(2) \sqrt{\frac{9}{8}\sqrt{3}}$
6	4	2	2	2	$(2) \sqrt{2}$
6	4	3	1	2	$(2) \sqrt{\frac{1}{2}\sqrt{6}}$
6	5	2	1	2	$(2) \sqrt{\frac{1}{2}\sqrt{5}}$
6	5	4	1	2	$(2) \sqrt{\frac{3}{4}\sqrt{6}}$
6	6	1	1	2	$(2) \sqrt{\frac{1}{2}\sqrt{3}}$
6	6	3	1	2	$(2) \sqrt{\frac{3}{4}\sqrt{5}}$
6	6	5	1	2	$(2) \sqrt{\frac{3}{4}\sqrt{10}}$

TABLE I. (Continued).

TABLE I. (Continued).

P_0	P_1	P_2	P_3	Dim.	$\lambda_{\beta_i} = \lambda_{\beta_i}(P_0, \dots, P_3)$
7	3	3	3	2	$(2)\sqrt{\frac{9}{8}\sqrt{3}}$
7	4	3	2	2	$(2)\sqrt{\frac{3}{4}\sqrt{6}}$
7	4	4	1	2	$(2)\sqrt{\frac{3}{2}}$
7	5	2	2	2	$(2)\sqrt{\frac{3}{4}\sqrt{5}}$
7	5	3	1	2	$(2)\sqrt{\frac{3}{8}\sqrt{15}}$
7	5	5	1	2	$(2)\sqrt{\sqrt{5}}$
7	6	2	1	2	$(2)\sqrt{\frac{3}{4}\sqrt{3}}$
7	6	4	1	2	$(2)\sqrt{\frac{5}{4}\sqrt{3}}$
7	6	6	1	2	$(2)\sqrt{\frac{1}{2}\sqrt{33}}$
7	7	1	1	2	$(2)\sqrt{\frac{3}{8}\sqrt{7}}$
7	7	3	1	2	$(2)\sqrt{\frac{1}{2}\sqrt{15}}$
7	7	5	1	2	$(2)\sqrt{\frac{3}{8}\sqrt{55}}$
7	7	7	1	2	$(2)\sqrt{2\sqrt{3}}$
8	4	3	3	2	$(2)\sqrt{\frac{3}{4}\sqrt{10}}$
8	4	4	2	2	$(2)\sqrt{\sqrt{5}}$
2	2	2	2	3	$(1)0, (2)\sqrt{\frac{1}{2}\sqrt{3}}$
3	3	2	2	3	$(1)0, (2)\sqrt{\frac{1}{4}\sqrt{26}}$
4	3	3	2	3	$(1)0, (2)\sqrt{\frac{3}{4}\sqrt{6}}$
4	4	2	2	3	$(1)0, (2)\sqrt{\frac{1}{2}\sqrt{11}}$
4	4	4	2	3	$(1)0, (2)\sqrt{\frac{3}{2}\sqrt{3}}$
5	3	3	3	3	$(1)0, (2)\sqrt{\frac{3}{2}\sqrt{3}}$
5	4	3	2	3	$(1)0, (2)\sqrt{\frac{1}{4}\sqrt{89}}$
5	5	2	2	3	$(1)0, (2)\sqrt{\frac{1}{4}\sqrt{66}}$
5	5	4	2	3	$(1)0, (2)\sqrt{\frac{1}{4}\sqrt{174}}$
6	4	3	3	3	$(1)0, (2)\sqrt{\frac{1}{4}\sqrt{174}}$
6	4	4	2	3	$(1)0, (2)\sqrt{3}$
6	5	3	2	3	$(1)0, (2)\sqrt{\frac{1}{4}\sqrt{131}}$
6	5	5	2	3	$(1)0, (2)\sqrt{\frac{1}{2}\sqrt{69}}$
6	6	2	2	3	$(1)0, (2)\sqrt{\frac{1}{2}\sqrt{23}}$
6	6	4	2	3	$(1)0, (2)\sqrt{\frac{3}{2}\sqrt{7}}$
6	6	6	2	3	$(1)0, (2)\sqrt{3\sqrt{3}}$

P_0	P_1	P_2	P_3	Dim.	$\lambda_{\beta_i} = \lambda_{\beta_i}(P_0, \dots, P_3)$
7	4	4	3	3	$(1)0, (2)\sqrt{\frac{1}{2}\sqrt{69}}$
7	5	3	3	3	$(1)0, (2)\sqrt{\frac{3}{2}\sqrt{7}}$
7	5	4	2	3	$(1)0, (2)\sqrt{\frac{1}{4}\sqrt{209}}$
7	6	3	2	3	$(1)0, (2)\sqrt{\frac{3}{2}\sqrt{5}}$
7	6	5	2	3	$(1)0, (2)\sqrt{\frac{1}{4}\sqrt{395}}$
7	7	2	2	3	$(1)0, (2)\sqrt{\frac{1}{4}\sqrt{122}}$
7	7	4	2	3	$(1)0, (2)\sqrt{\frac{3}{4}\sqrt{38}}$
7	7	6	2	3	$(1)0, (2)\sqrt{\frac{3}{2}\sqrt{17}}$
3	3	3	3	4	$(2)\sqrt{\frac{3}{8}\sqrt{3}},$ $(2)\sqrt{\frac{3}{8}\sqrt{35}}$
4	4	3	3	4	$(2)\sqrt{\frac{3}{4}\sqrt{9-57}},$ $(2)\sqrt{\frac{3}{4}\sqrt{9+57}}$
5	4	4	3	4	$(2)\sqrt{\frac{3}{8}\sqrt{66-2\sqrt{753}},}$ $(2)\sqrt{\frac{3}{8}\sqrt{66+2\sqrt{753}}}$
5	5	3	3	4	$(2)\sqrt{\frac{1}{8}\sqrt{511-16\sqrt{721}},}$ $(2)\sqrt{\frac{1}{8}\sqrt{511+16\sqrt{721}}}$
5	5	5	3	4	$(2)\sqrt{\sqrt{3}},$ $(2)\sqrt{\sqrt{30}}$
6	4	4	4	4	$(2)\sqrt{\sqrt{3}},$ $(2)\sqrt{\sqrt{30}}$
6	5	4	3	4	$(2)\sqrt{\frac{1}{8}\sqrt{918-18\sqrt{1801}},}$ $(2)\sqrt{\frac{1}{8}\sqrt{918+18\sqrt{1801}}}$
6	6	3	3	4	$(2)\sqrt{\frac{1}{4}\sqrt{183-3\sqrt{2641}},}$ $(2)\sqrt{\frac{1}{4}\sqrt{183+3\sqrt{2641}}}$
6	6	5	3	4	$(2)\sqrt{\frac{1}{8}\sqrt{1602-18\sqrt{5281}},}$ $(2)\sqrt{\frac{1}{8}\sqrt{1602+18\sqrt{5281}}}$
7	6	4	3	4	$(2)\sqrt{\frac{3}{4}\sqrt{6}},$ $(2)\sqrt{\frac{3}{4}\sqrt{66}}$
7	7	7	3	4	$(2)\sqrt{\frac{15}{8}\sqrt{3}},$ $(2)\sqrt{\frac{3}{8}\sqrt{715}}$

TABLE II. The eigenvalues of the volume for some five-valent vertices.

P_0	P_1	P_2	P_3	P_4	Dim.	$\lambda_{\beta_i} = \lambda_{\beta_i}(P_0, \dots, P_4)$
2	1	1	1	1	3	(3) $\sqrt{\frac{3\sqrt{2} + \sqrt{3}}{12}}$
2	2	2	1	1	4	(2) $\sqrt{\frac{29\sqrt{2} + 12\sqrt{3} + 16\sqrt{5}}{96}},$ (1) $\sqrt{\frac{5\sqrt{2} + 4\sqrt{5}}{16}},$ (1) $\sqrt{\frac{5\sqrt{2} + 4\sqrt{5}}{24}}$
2	2	2	2	2	6	(6) $\sqrt{\frac{5}{3}}\sqrt{3}$
3	2	1	1	1	3	(2) $\sqrt{\frac{21\sqrt{2} + 6\sqrt{3} + 18\sqrt{5} + 14\sqrt{15}}{192}},$ (1) $\sqrt{\frac{15\sqrt{2} + 18\sqrt{5} + 4\sqrt{15}}{96}}$
4	2	2	1	1	3	(1) $\sqrt{\frac{40 + 10\sqrt{2} + 4\sqrt{5} + 5\sqrt{6}}{80}}$ (1) $\sqrt{\frac{60 + 15\sqrt{2} + 20\sqrt{3} + 12\sqrt{5} + 10\sqrt{6}}{160}}$ (1) $\sqrt{\frac{20 + \sqrt{2} + 4\sqrt{3} + 4\sqrt{5}}{32}}$

- [1] R. Penrose, in *Magic Without Magic: John Archibald Wheeler*, edited by J. R. Klauder (W. H. Freeman and Company, San Francisco, 1972).
- [2] C. Rovelli and L. Smolin, Phys. Rev. Lett. **61**, 1155 (1988).
- [3] C. Rovelli and L. Smolin, Nucl. Phys. **B331**, 80 (1990).
- [4] C. Isham, *Structural Issues in Quantum Gravity*, to appear in the proceedings of the GR14 (Florence 1995).
- [5] *Diffeomorphism Invariant Quantum Field Theory and Quantum Geometry* [J. Math. Phys. **36** (1995)].
- [6] J. Baez, *Knots and Quantum Gravity* (Oxford University Press, Oxford, 1994).
- [7] J. Ehlers and H. Friedrich, *Canonical Gravity: from Classical to Quantum* (Springer-Verlag, Berlin, 1994).
- [8] C. Rovelli, Class. Quantum Grav. **8**, 1613 (1991).
- [9] A. Ashtekar, in *Gravitation and Quantization, Les Houches*, Proceedings of the Les Houches Summer School, Les Houches, France, 1992, edited by B. Julia and J. Zinn-Justin, Les Houches Summer School Proceedings Vol. 57 (Elsevier, Amsterdam, 1995).
- [10] L. Smolin, in *Brill Festschrift Proceedings*, edited by B. Hu and T. Jacobson (Cambridge University Press, Cambridge, England, 1993); *Quantum Gravity and Cosmology* (World Scientific, Singapore, 1993).
- [11] R. Gambini and J. Pullin, *Loops, Knots, Gauge Theories and Quantum Gravity* (Cambridge University Press, Cambridge, England, 1996).
- [12] B. Brüggmann, in [7], p. 213.
- [13] K. Ezawa, "Nonperturbative solutions for canonical quantum gravity: an overview," Report No. gr-qc/9601050 (unpublished).
- [14] A. Ashtekar and C. Isham, Class. Quantum Grav. **9**, 1433 (1992).
- [15] A. Ashtekar, J. Lewandowsky, D. Marolf, J. Mourao, and T. Thiemann, J. Math. Phys. **36**, 6456 (1995).
- [16] A. Ashtekar and J. Lewandowski, "Quantum Theory of Geometry: Area Operator," Report No. gr-qc/9602046 (unpublished).
- [17] J. Lewandowski, "Volume and Quantization," report, 1996 (unpublished).
- [18] R. De Pietri, "On the relation between the connection and the loop representation of quantum gravity," University of Parma Report No. UPRF-96-466, 1996 (unpublished).
- [19] C. Rovelli and L. Smolin, Phys. Rev. D **52**, 5743 (1995).
- [20] J. C. Baez, Adv. Math. **117**, 253 (1996); *Spin Networks in Nonperturbative Quantum Gravity*, in *The Interface of Knots and Physics*, edited by L.H. Kauffman (American Mathematical Society, Providence, RI, 1996).
- [21] T. Foxon, Class. Quantum Grav. **12**, 951 (1995).
- [22] A. Ashtekar, C. Rovelli, and L. Smolin, Phys. Rev. Lett. **69**, 237 (1992).
- [23] C. Rovelli and L. Smolin, Nucl. Phys. **B442**, 593 (1995).
- [24] R. Loll, Phys. Rev. Lett. **75**, 3048 (1995); A. Ashtekar and J. Lewandowski, J. Geom. Phys. **17**, 191 (1995); J. Lewandowski, lecture given at the Workshop on Canonical and

- Quantum Gravity, Warsaw, 1995 (unpublished).
- [25] C. Rovelli, Nucl. Phys. **B405**, 797 (1993).
- [26] C. Rovelli and L. Smolin, Phys. Rev. Lett. **72**, 446 (1994); R. Borissov, “Graphical Evolution of Spin Network States” (in preparation); R. Gambini and J. Pullin, “A rigorous solution of the quantum Einstein equations,” Report No. gr-qc/9511042 (unpublished); “The general solution of the quantum Einstein equations?” Report No. gr-qc/9603019 (unpublished).
- [27] C. Rovelli, J. Math. Phys. **36**, 6529 (1995).
- [28] C. Rovelli and H. Morales-Tecotl, Phys. Rev. Lett. **72**, 3642 (1994); Nucl. Phys. **B451**, 325 (1995).
- [29] K. Krasnov Phys. Rev. D **53**, 1874 (1996).
- [30] R. Gambini and J. Pullin, Phys. Rev. D **47**, R5214 (1993).
- [31] R. Penrose, in *Combinatorial Mathematics and its Application*, edited by D. Welsh (Academic Press, New York, 1971).
- [32] L. H. Kauffman and S. L. Lins, *Temperley-Lieb Recoupling Theory and Invariant of 3-Manifolds* (Princeton University Press, Princeton, NJ, 1994).
- [33] M. Reisenberger, “Spin-network states and operators” (in preparation).
- [34] S. Major and L. Smolin, “Quantum deformation of quantum gravity” Report No. CGPG-95/12-3 (1995), gr-qc/9512020 (unpublished); R. Borissov, S. Major, and L. Smolin, “The geometry of quantum spin networks,” Report No. CGPG-95/12-4 (1995), gr-qc/9512043 (unpublished).
- [35] R. Borissov, “Eigenvalue spectrum of the Volume Operator in Quantum Gravity” (in preparation).
- [36] R. Loll, Nucl. Phys. **B460**, 143 (1996).
- [37] J. F. Barbero, Phys. Rev. D **51**, 5507 (1995).
- [38] A. Ashtekar, Phys. Rev. Lett. **57**, 2244 (1986); Phys. Rev. D **36**, 1587 (1987); for an introduction to the Ashtekar formalism, see Ref. [8], or A. Ashtekar, *Nonperturbative Canonical Gravity* (World Scientific, Singapore, 1991).
- [39] T. Thiemann, Class. Quantum Grav. **13**, 1383 (1996); A. Ashtekar, Phys. Rev. D **53**, 2865 (1996).
- [40] R. Loll, Phys. Rev. D (to be published).
- [41] G. Immirzi, “Quantizing Regge Calculus,” Report No. gr-qc/9512040 (unpublished).
- [42] S. Major (private communication).
- [43] R. Penrose, in *Quantum Theory and Beyond*, edited by T. Bastin (Cambridge University Press, Cambridge, England, 1971).
- [44] C. Rovelli, T. Newman, and J. Lewandowski, J. Math. Phys. **34**, 4646 (1993).
- [45] R. Gambini and A. Trias, Nucl. Phys. **B278**, 436 (1986); Phys. Rev. D **23**, 553 (1981).
- [46] L. H. Kauffman, in *Knots, Topology and Quantum Field Theories*, edited by L. Lusanna (World Scientific, Singapore, 1991).
- [47] M. Behzad and G. Chartrand, *Introduction to the Theory of Graphs* (Allyn and Bacon, Boston, 1971).
- [48] K. Reidemeister, *Knotentheorie* (Springer, Berlin, 1932).
- [49] B. Brügmann, R. Gambini, and J. Pullin, Phys. Rev. Lett. **68**, 431 (1992); Nucl. Phys. **B385**, 587 (1992); Gen. Relativ. Gravit. **25**, 1 (1993); B. Brügmann, in *Canonical Gravity: From Classical to Quantum*, edited by J. Ehlers and H. Friedrich (Springer-Verlag, Berlin, 1993); J. Pullin, in *Proceedings of the Vth Mexican School of Particles and Fields*, edited by J. Lucio (World Scientific, Singapore, 1993).
- [50] C. Rovelli, Phys. Rev. D **47**, 1703 (1993).
- [51] S. Frittelli, L. Lehner, and C. Rovelli, “The Complete Spectrum of the Area from Recoupling Theory in Loop Quantum Gravity,” report (unpublished).
- [52] D. M. Brink and G. R. Satchler, *Angular Momentum* (Clarendon Press, Oxford, 1968).
- [53] A. Ashtekar and J. Lewandowski, in [6], p. 21.
- [54] C. Rovelli, Class. Quantum Grav. **8**, 297 (1991); **8**, 317 (1991).
- [55] J. Iwasaki and C. Rovelli, Int. J. Mod. Phys. D **1**, 533 (1993); Class. Quantum Grav. **11**, 1653 (1994).
- [56] S. Hawking, Commun. Math. Phys. **43**, 199 (1975).
- [57] M. Barreira, M. Carfora, and C. Rovelli, “Physics with non-perturbative quantum gravity: radiation from a quantum black hole,” Report No. gr-qc/9603064 (unpublished).
- [58] C. Rovelli, “Black Hole Entropy from Loop Quantum Gravity,” Report No. gr-qc/9603063 (unpublished).
- [59] L. H. Kauffman, Trans. Am. Math. Soc. **318**, 417 (1990).
- [60] Moussoris, in *Advances in Twistor Theory, Research Notes in Mathematics*, edited by Huston and Ward (Pitman, New York, 1979), pp. 308–312.
- [61] L. H. Kauffman, Int. J. Mod. Phys. A **5**, 93 (1990).
- [62] I. Levinson, Liet. TSR Mokslu Akad. Darb. **B4**, 3 (1956).
- [63] A. P. Yutsin, J. B. Levinson, and V. V. Vanagas, *Mathematical Apparatus of the Theory of Angular Momentum* (Israel program for Scientific Translation, Jerusalem, 1962).